REPUBLIQUE DU BURUNDI
Institute Geographique du Burundi
(IGEBU)
Gitega

BUNDESREPUBLIK
DEUTSCHLAND
Bundesanstalt für Geowissenschaften
und Rohstoffe (BGR)
Hannover

Burundi – Management and Protection of Groundwater Resources

Lineament mapping for the localisation of high groundwater potential

using remote sensing

Dr. Kai Hahne

Hannover, December 2014

Lineament mapping for the localisation of high groundwater potential using remote sensing

Author	Dr. Kai Hahne (BGR)
Commissioned by	Federal Ministry for Economic Cooperation and Development (BMZ: Bundesministerium für wirtschaftliche Zusammenarbeit und Entwicklung)
Project Number	BMZ PN 2009.2040.5
BGR Number	05-2348
Implementing Agencies	MEEATU (Ministère de l'Eau, de l'Environnement, de l'Aménagement du Territoire et de l'Urbanisme); IGEBU (Institut Géographique du Burundi)
	Federal Institute for Geosciences and Natural Resources (BGR: Bundesanstalt für Geowissenschaften und Rohstoffe, Hannover)
Pages	61
Place and date of issuance	Hannover, December 2014

Table of Contents

Abbreviations

ASTER GDEM	Advanced Spaceborne Thermal Emission and Reflection Radiometer Global Digital Elevation Map. (Digital Elevation Model; combination of ASTER-Satellite data and SRTM data)
BGR	Bundesanstalt für Geowissenschaften und Rohstoffe (Federal Institute for Geosciences and Natural Resources)
DEM	Digital Elevation Model
GIS	Geographic Information System
GPS	Global Positioning System
IGEBU	Institute Geographique du Burundi (Cooperation partner)
m asl	Metres above sea level
Pmax	Maximum principal stress
Pmin	Minimum principal stress
RGB	Red Green Blue (colour band combination)
SPOT	Satellite Pour l´Observation de la Terre
SRTM	Shuttle Radar Topography Mission
TEM	Transient Electromagnetics (Geophysical measurement method)
TM	Thematic Mapper (Sensor on board of Landsat satellite)
WP	Way Point (Measured by GPS)

List of figures and table

Summary

Within crystalline and metamorphic rocks, faults and joints represent the main pathways for groundwater migration. Especially steep to medium dipping structures can be detected at the earth´s surface as lineaments.

A lineament mapping survey was conducted in three different working areas, using high- and medium resolution multispectral satellite images (SPOT, Landsat TM).

The resulting maps are significantly more detailed than older lineament maps (BARRAT, JM ET AL. 2011). Lineaments were classified in four categories, where “Category 4” represents the smallest surface expression. Lineaments of this category are only visible in enhanced satellite images and not detectable in the field. They represent the majority of all mapped lineaments. Considering this fact, the importance for using remote sensing techniques becomes obvious.

Lineament directions are various but NE-SW and NW-SE are dominant all over the working areas. They are related to young and active rift tectonics, which appear to (re-) activate older Kibaran structures at many locations. At most sites they are found to be open for groundwater migration. Highest groundwater potential is expected at intersections of different lineament directions. This is proven at locations with existing wells and also at new drilling sites.

Because most of the lineaments appear to be open flow paths for groundwater migration, contamination can take place along these vectors as well. Pit latrines seem to be the most relevant factor for bacterial groundwater contamination.

1 Scope of the Work

Within the bilateral project "Burundi – Management and Protection of Groundwater Resources" between BGR and the "Institute Geographique du Burundi" (IGEBU), one focus lies upon groundwater quality and its vulnerability to pollution.

Existent wells are mainly situated at valley bottoms. In most cases they are highly bacteria-contaminated at these locations due to lacking waste water infrastructure. Alternative drilling sites located uphill have to be determined where a better drinking water quality can be assumed.

Existing lineament maps (BARRAT, JM ET AL. 2011) are poor in resolution and not sufficient to meet the requirements of the project. By using multispectral remote sensing data of high- and medium ground resolution, a higher number of lineaments can be detected with more detailed characterisation.

Field work was conducted from 04/10/2012 to 26/10/2012. Preliminary results have been presented and discussed with the BGR-IGEBU project team as well as with parts of IGEBU directorate and external audience (Consultants, drilling engineers and leading staff of local water supply) at the end of the mission.

2 Working Areas

Three working areas were defined (Fig. 2.1):

1. In the north around Kirundo (Fig. 2.2) and close to the border of Rwanda.
2. Around Gitega in the centre of Burundi (Fig. 2.3) and - at short notice -
3. Around Rumonge in the southwest of the country at Lake Tanganyika (Fig. 2.4).

Although satellite data of Rumonge had a coarser ground resolution (30m x 30m) than the other images, lineament mapping was successful.

The whole project area consists of different crystalline basement rocks with no porosity. Under these geological preconditions, groundwater migration can only take place along existing joints, cleavage and faults. Most of these structures can be detected at the earth´s surface via remote sensing techniques as lineaments. Lineament cross points and areas of high lineament density suggest areas of high groundwater potential for drilling purposes.

Due to a thick soil cover at most places of the working areas (around Kirundo 100 m weathered granite, personal communication Ch. Tiberghien), the usage of multispectral remote sensing data (Landsat TM, SPOT) and -methods is most valuable for a lineament detection in an extensive area. Furthermore, it is possible to detect structures, which are invisible using ground-bound field work only.

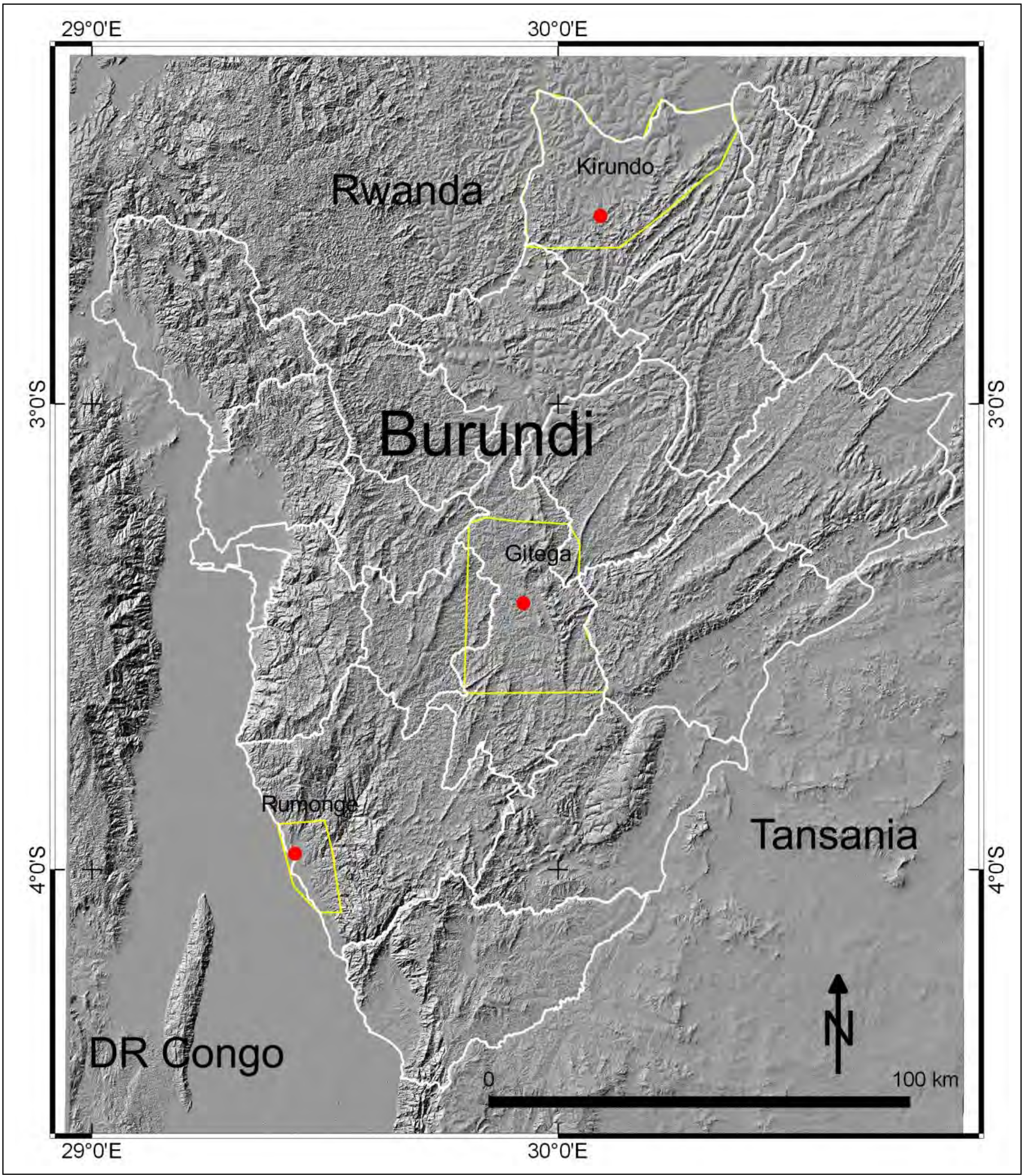

Figure 2.1: Location of the working areas (yellow frames) in Burundi (provinces white frames) with neighbouring countries projected onto ASTER GDEM elevation model.

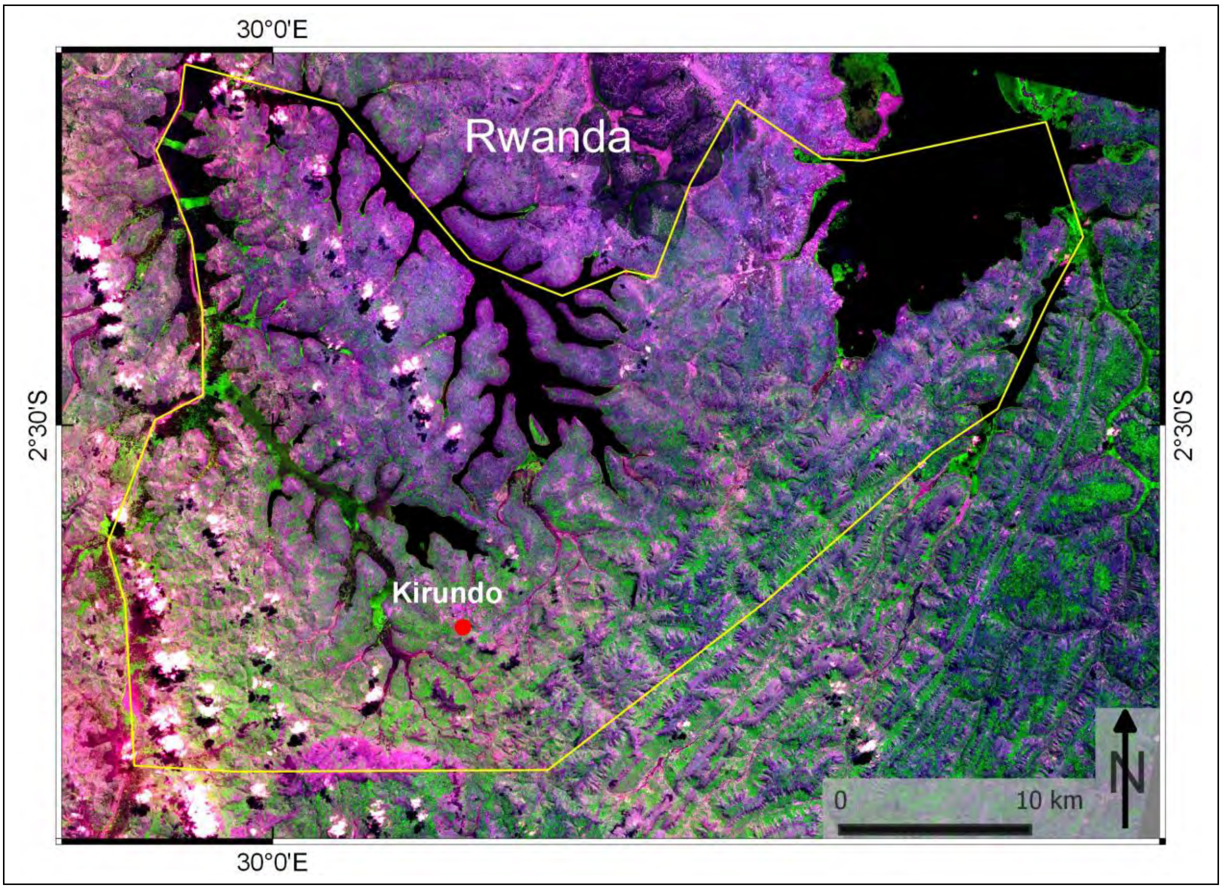

Figure 2.2: Working area 1 in Kirundo province. Projected onto SPOT bands 2,3,1 (RGB).

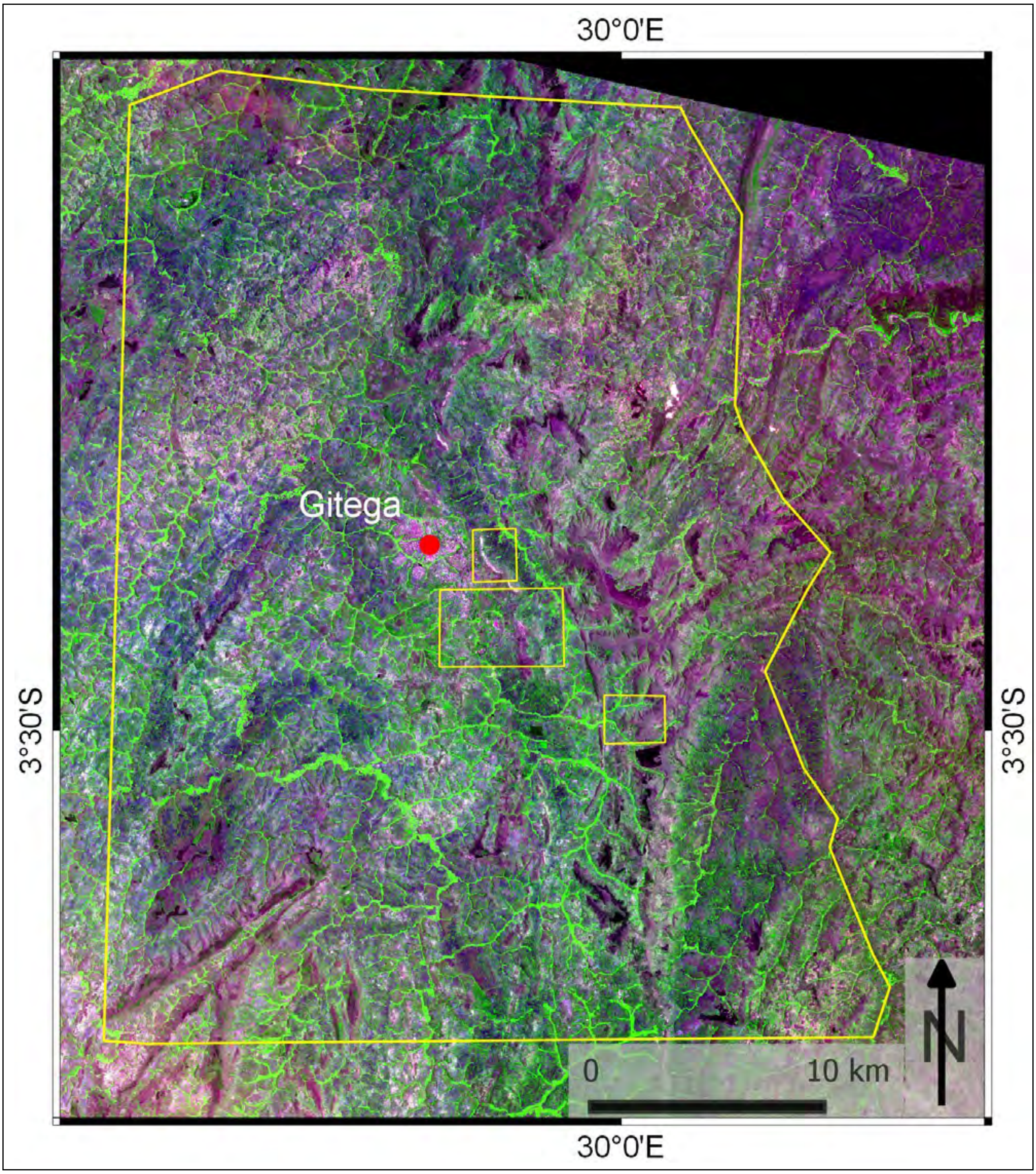

Figure 2.3: Working area 2 in Gitega province. Yellow rectangles mark areas of special interest. Projected onto SPOT bands 2,3,1 (RGB).

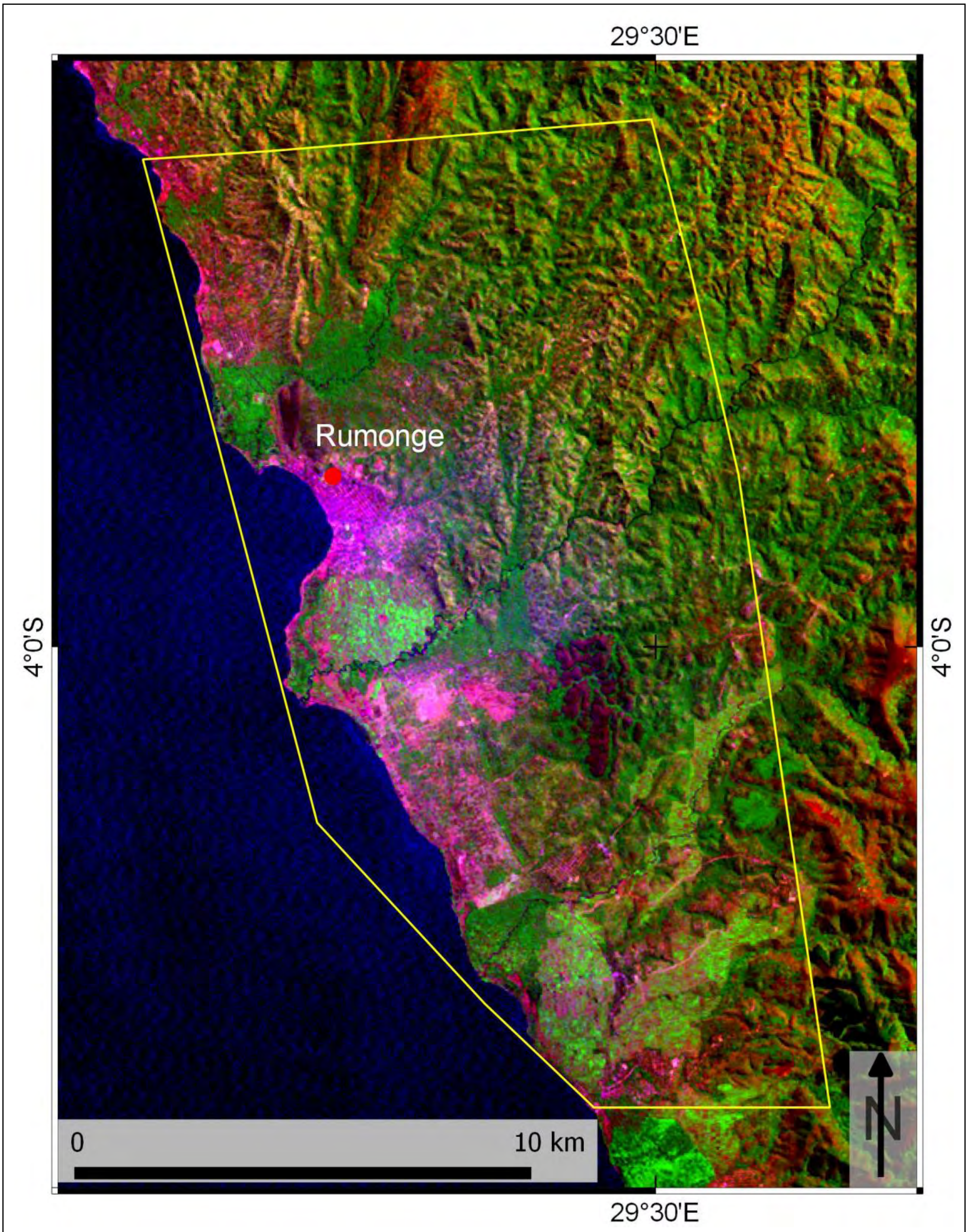

Figure 2.4: Working area 3 around the town of Rumonge. Projected onto Landsat TM image, bands 7,4,1 (RGB).

3 Data

The following data are used within Quantum GIS (version 2.4) for further analysis and lineament vectorization:

- Enhanced and geocoded satellite images:
    - SPOT acquired August, 08, 2009 (Kirundo), September, 26, 2007 (Gitega)
    - Landsat TM acquired July, 24, 2011 (Rumonge)
    - Aster GDEM digital elevation model
- Geocoded raster data:
    - Geological maps
        - Map Sheet, S3/29 NE, S3/30 NW and S3/30 NE, Busoni (Karayenga, 1989)
        - Map Sheet S3/30-SW, Muyinga (CLAESSENS, W. ET KARAYENGA, D. 1986),
        - Map Sheet, S4/29 NE, Gitega (CLAESSENS, W. ET THEUNISSEN, K., 1988):
        - Map Sheet, S4/29 SW, Rumonge (THEUNISSEN, K., 1986)
- Information from field work:
    - Shape and visibility of lineaments
    - Additional geological and tectonic information
    - Dip/strike of foliation and joints where measurements were possible
    - Field photos
    - Waypoints (WP) from GPS measurements.

Coordinates of all locations surveyed in the field are taken with GPS (Garmin 60 CSx, average accuracy of +/- 5 m). This information was entered into GIS tables.

The spatial reference system used for this study is UTM 36 S, WGS 84

The following layers have been created:

- Lineaments SPOT Kirundo (categorised)
- Lineaments SPOT Gitega (categorised)

- Lineaments TM Rumonge (categorised)
- Waypoints with corresponding data tables concerning information from field work (lithology, photos etc.)

The data including additional field photos, are attached on DVD to this report as a Quantum GIS-project. In figures, that show field photos, the location refers to a GPS waypoint (WP). All waypoints are listed in a table in the appendix.

4 Geology

4.1 Precambrian

The geology of Burundi consists almost entirely of Precambrian rocks (Figures 4.11-4.13). To the west it is underlain by Metasediments and Granites which belong to the Ubedian orogenesis, 1600-2200 m.y. (V. DEN HAUTE, 1984). In the central- and eastern part the rocks are attributed to the Kibaran fold belt, 900-1400 m.y. This orogenesis was accompanied by intense granitic and basic magmatism (V. DEN HAUTE, 1984). Metamorphic rock types occur as Quartzites, Schists and Gneisses (Figures 4.1 to 4.6). Metamorphic grade varies between low grade (greenschist facies) in the east towards higher grade (granulite facies) in the west (RUMVEGERI, B. T., 1991).

Figure 4.1: Amphibolitic gneiss in a building pit north of Rumonge (WP 83).

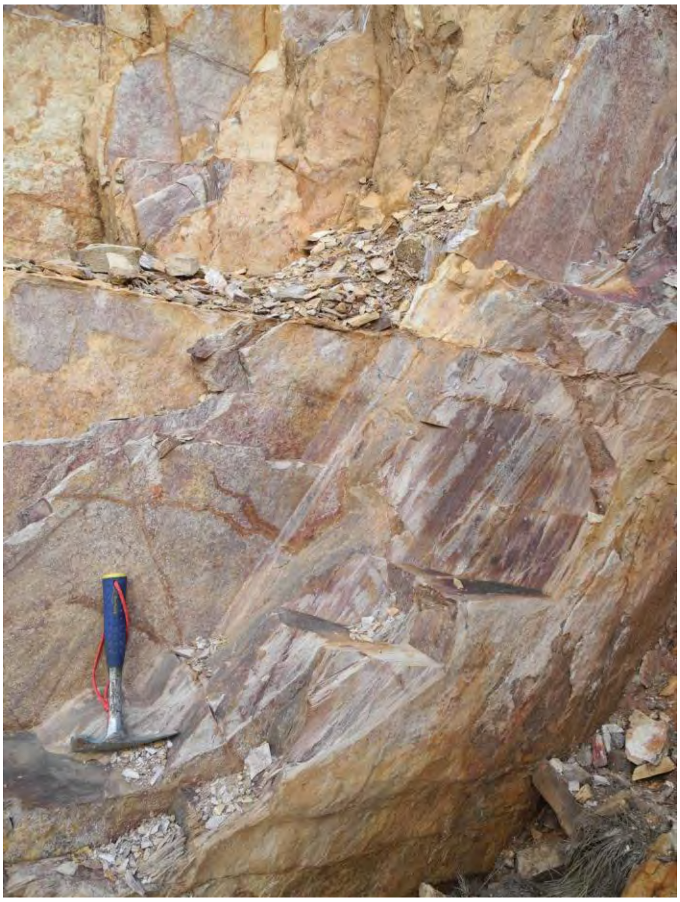

Figure 4.2: Fine pinkish Quartzite east of Gitega (WP 53).

Figure 4.3: Coarse undeformed Quartzite north of Kirundo (WP 01).

Figure 4.4: Quartzite with cataclastic texture north of Kirundo close to Rwandan border (WP 52).

Figure 4.5: Mica schist with graphite. Location north of Kirundo (WP 21).

Figure 4.6: Tall Mica and Quartz crystals of a pegmatitic vein. Location north of Kirundo (WP 29).

4.2 Cenozoic

The observed Cenozoic sediments are limited to alluvial fill of valley bottoms, pediments at slopes, terraces at Lake Tanganyika and the development of various soils, particularly Laterite (Figures 4.7 to 4.10).

Thick soil covers most rocks in the working areas. In the vicinity of Kirundo 100 m of intensive weathered granitic substrate is proven (personal communication, Ch. Tiberghien).

Figure 4.7: Left: Soil development (with holes from roots) on pegmatitic substrate. Right: altered pegmatite. Locations north of Kirundo (WP 40).

Figure 4.8: Left: thick soils in valley bottoms are used for the production of bricks. Right: Simple oven for the brick production. Both locations situated east of Gitega.

Figure 4.9: Pisolithic laterite crust. Location north of Kirundo (WP 15).

Figure 4.10: Left: thick iron oxide crust (WP 29). Right: Iron concretions (WP 21) genesis by intensive tropical alteration. Both locations are situated north of Kirundo.

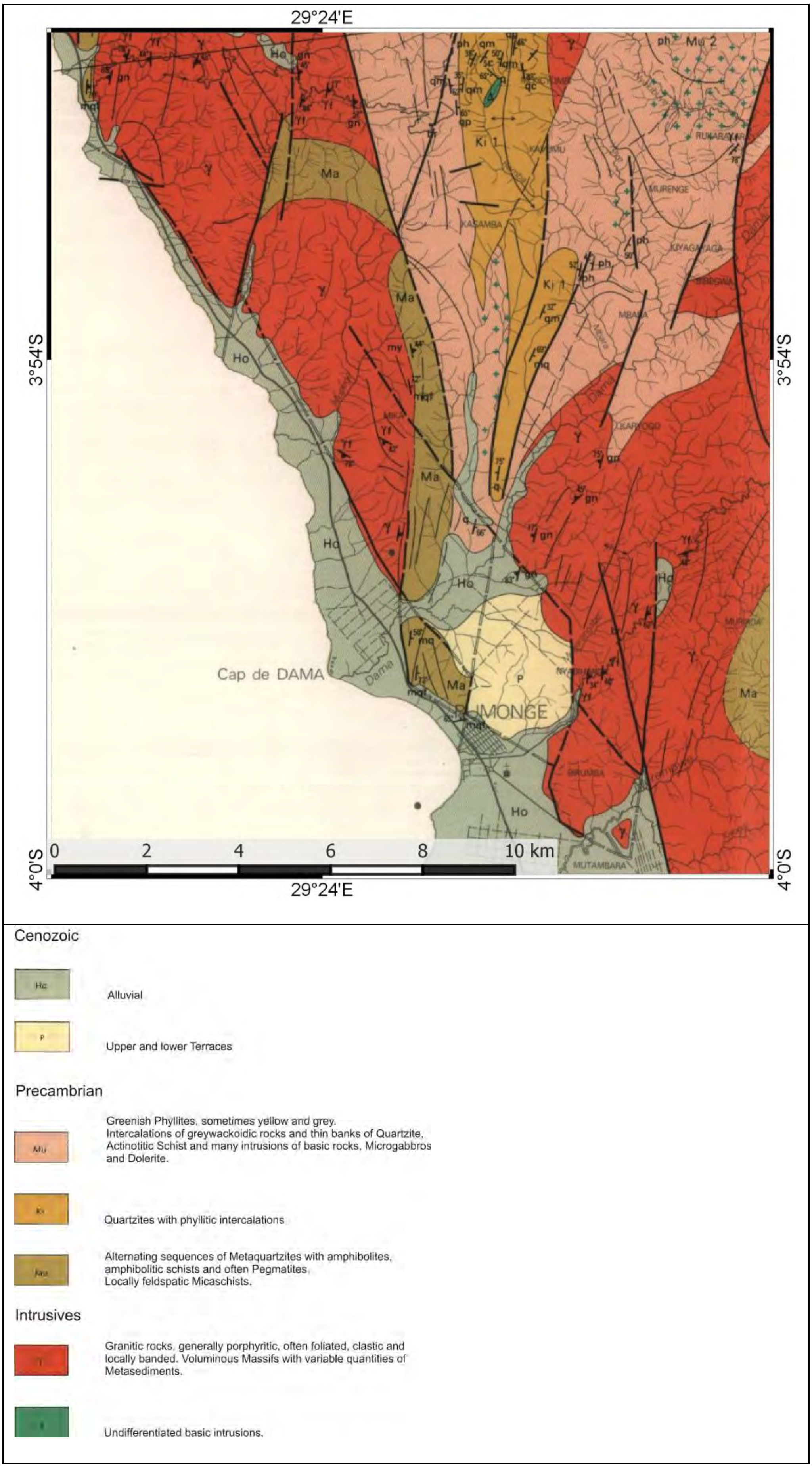

Figure 4.11: Subset of the Geological Map of Rumonge, THEUNISSEN, K. (1986).

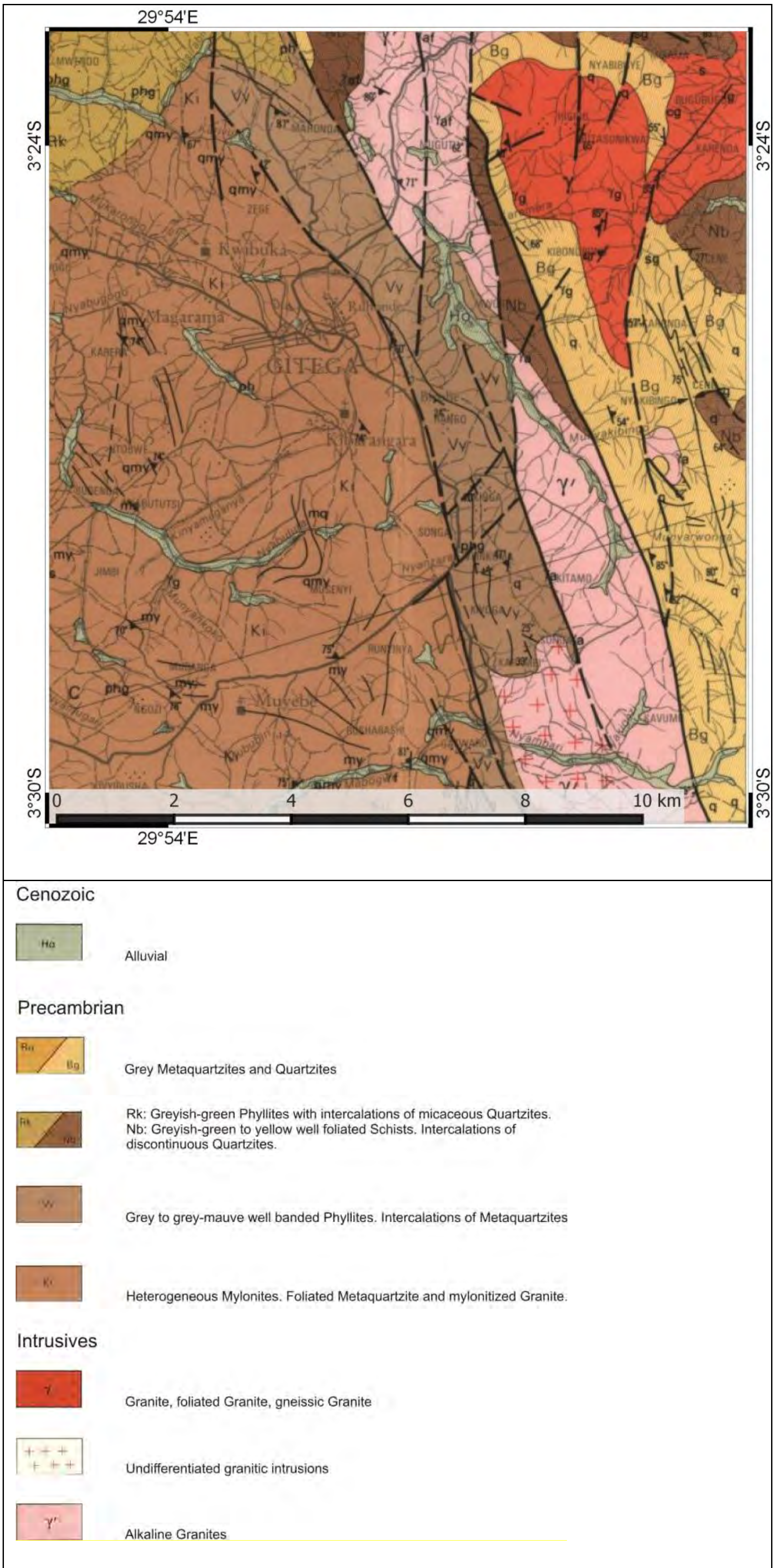

Figure 4.12: Subset of the Geological Map of Gitega, CLAESSENS, W. AND THEUNISSEN, K. (1988).

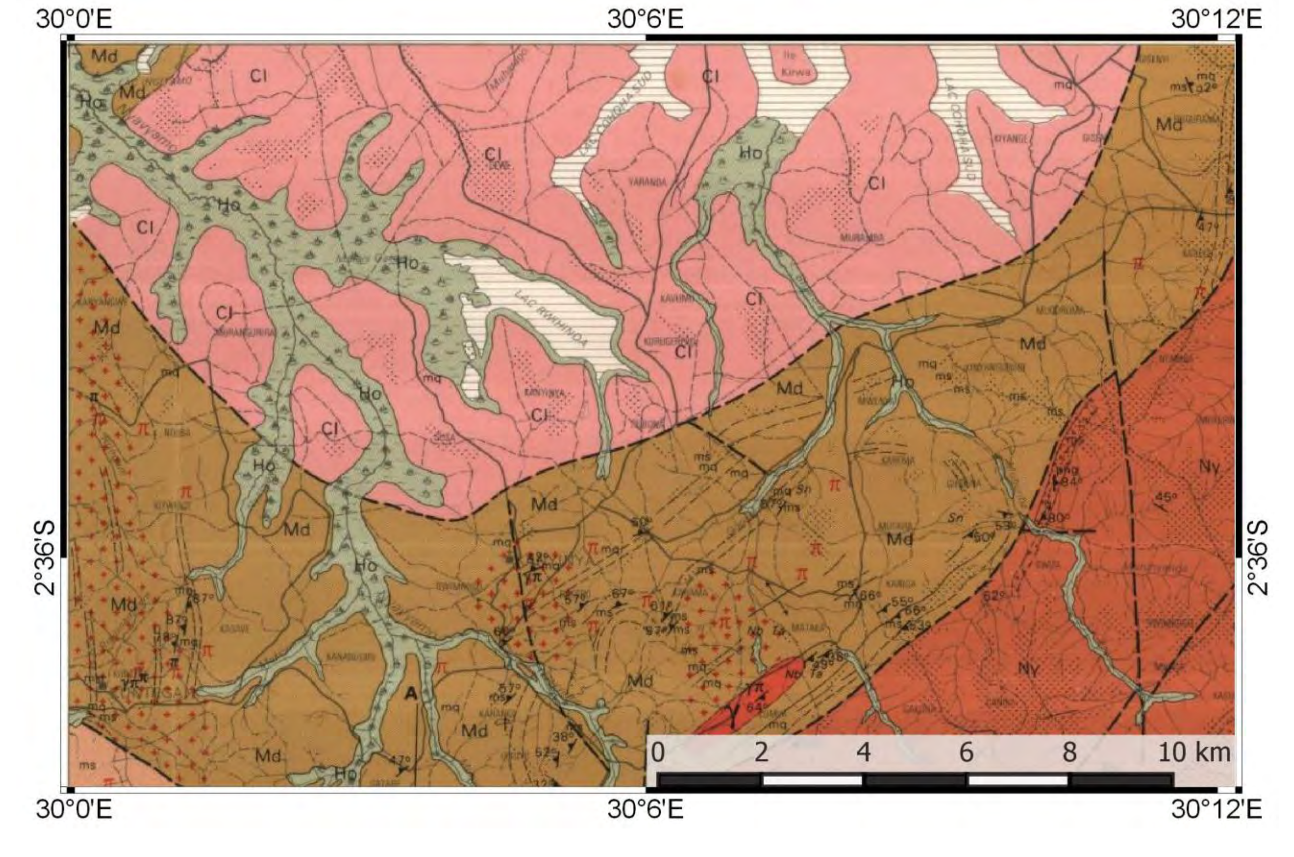

Cenozoic

Ho — Alluvial

Precambrian

Ny — Arenitic Schists and greyish Schists with intercalations of Quartzites and Microkonglomerates of sedimentary structure.

Md — Quartzitic Metasediments with Tourmaline. Banks of very fine grey Quartzite often pyritic with cataclastic texture.

Cl — Granitic and quartzitic area. Probably formed by Granites and Pegmatites and accessorial by Metasediments.

Intrusives

$\gamma\pi$ — Micaceous pegmatitic Granite

γ — Porphyritic Granite with two micas

Figure 4.13: Subset of the Geological Map of Muyinga (Kirundo), CLAESSENS, W. AND KARAYENGA, D. (1986).

5 Tectonic setting

The major part of Burundi is built up of lithological units of the Precambrian Kibara Belt. As this structure is not continuous along its total length, the north eastern part of this belt was re-named to Karagwe-Ankole Belt (TACK, L. ET. AL., 2010). Its main structural trend is NE-SW.

Lake Tanganyika represents an active rift and is part of a major right lateral fault zone (Fig. 5.1) which is linked with the reactivated Kibaran shear zone (CHOROVICZ, J. ET AL. 1990).

Around the area of Rumonge the rift direction of Lake Tanganyika becomes clear on satellite images by the expression of x-shaped stress indicators which are formed by conjugate fault systems (Fig. 5.2).

The acute angle between conjugate faults is bisected by the maximum principal stress direction (Pmax). The direction of the effective minimum principal stress (Pmin, perpendicular to Pmax) corresponds to the opening direction of the rift (Fig. 5.2).

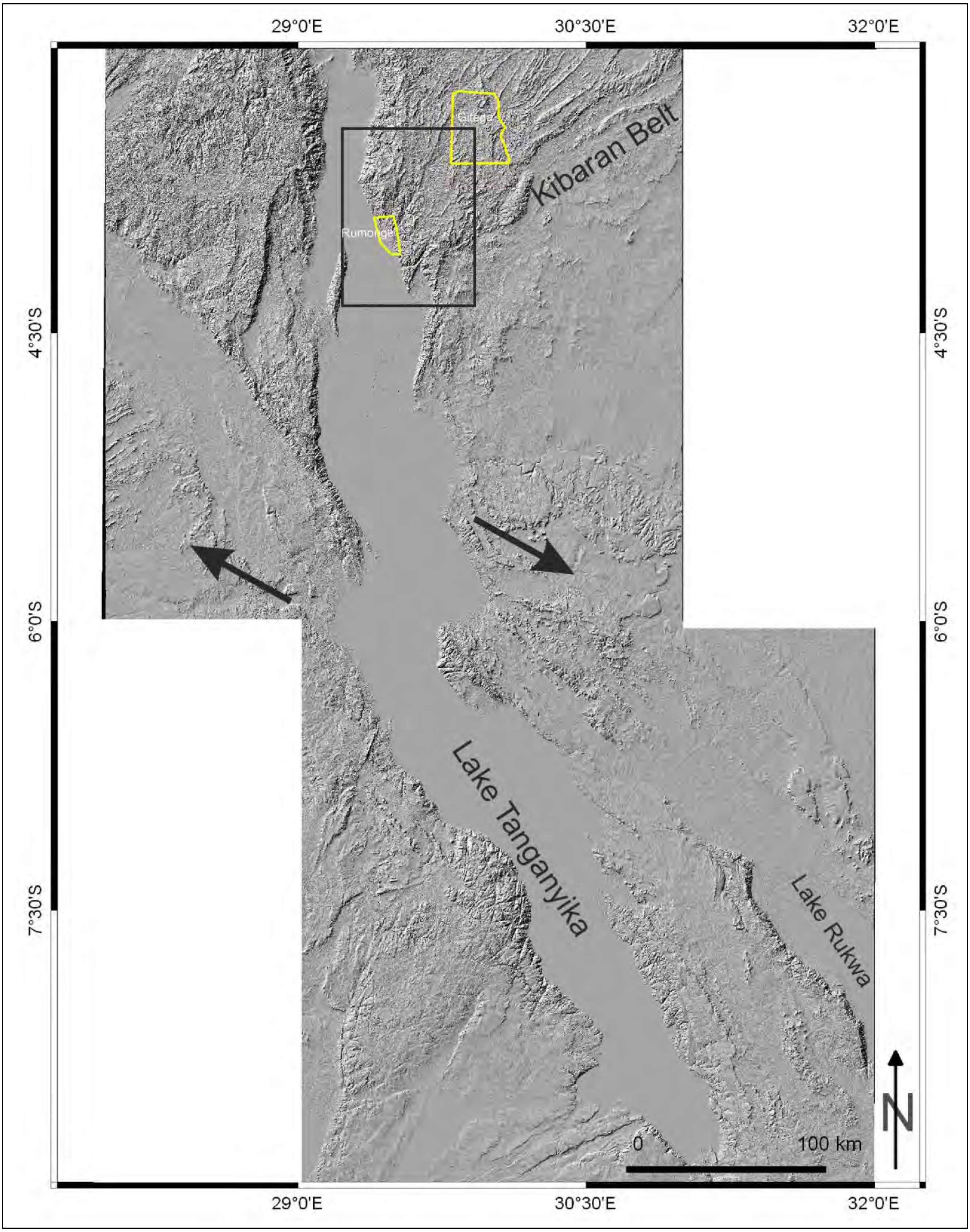

Figure 5.1: Lake Tanganyika represents an active rift. It is part of a major right lateral fault zone. The direction of opening (black arrows) is visible by simply considering the western- and eastern shore lines of the central lake and becomes additionally obvious by well-developed x-shaped stress indicators (rectangle see closer view in next fig.). In the North, a part of the Kibaran Belt is visible. Yellow polygons: working areas Rumonge and Gitega. Image: ASTER GDEM, shaded relief.

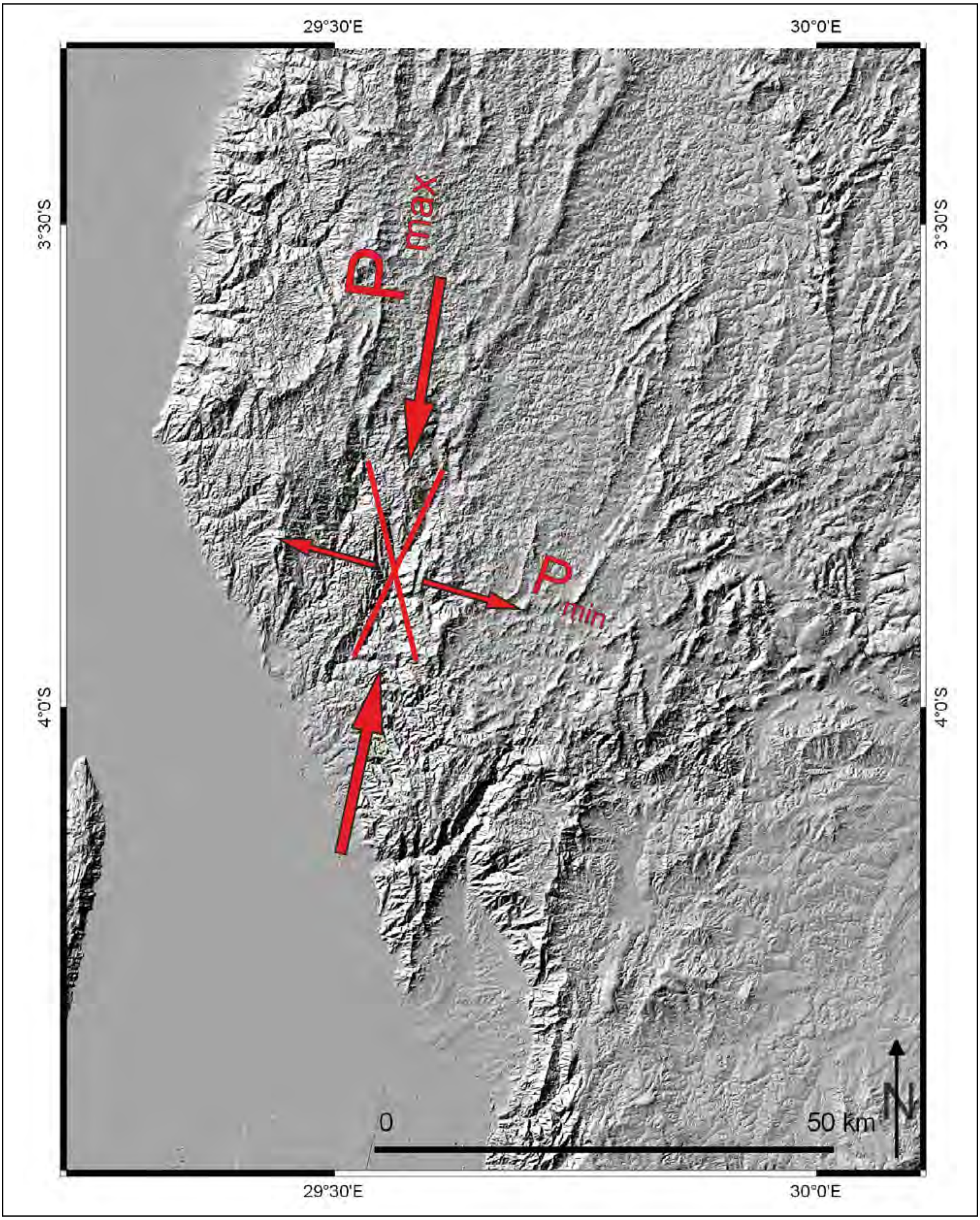

Figure 5.2: Close up of the area defined by the rectangle in fig. 5.1. The directions of maximum principal stress can be derived from satellite imagery, regarding the X-shaped stress indicators (red lines). The acute angle between conjugate faults (red lines, one example of plenty existing) is bisected by the maximum principal stress direction (Pmax). The direction of effective Pmin corresponds to the direction of the opening rift.

5.1 Faults/Joints

Rumonge:

Coast parallel lineaments belong to a system of conjugate faults (Fig. 5.2) striking NE (040°-060°, subordinate 010°-025°) and SE (135°-170°). They express a relatively young tectonic movement, which is strongly connected to rifting. The young age of the movement becomes obvious, as Cenozoic and Quaternary sediments are affected as well as the basement rocks (Fig. 5.4).

Where young sediments are present closer to the shore, they overlay the basement rocks (metamorphites and granites). The increasing thickness of the sedimentary layers towards Lake Tanganyika is shown very clear in a recent TEM measurement profile. It reveals strong evidence for the developing rift structure (Fig. 5.3, NOELL, U. (2014).

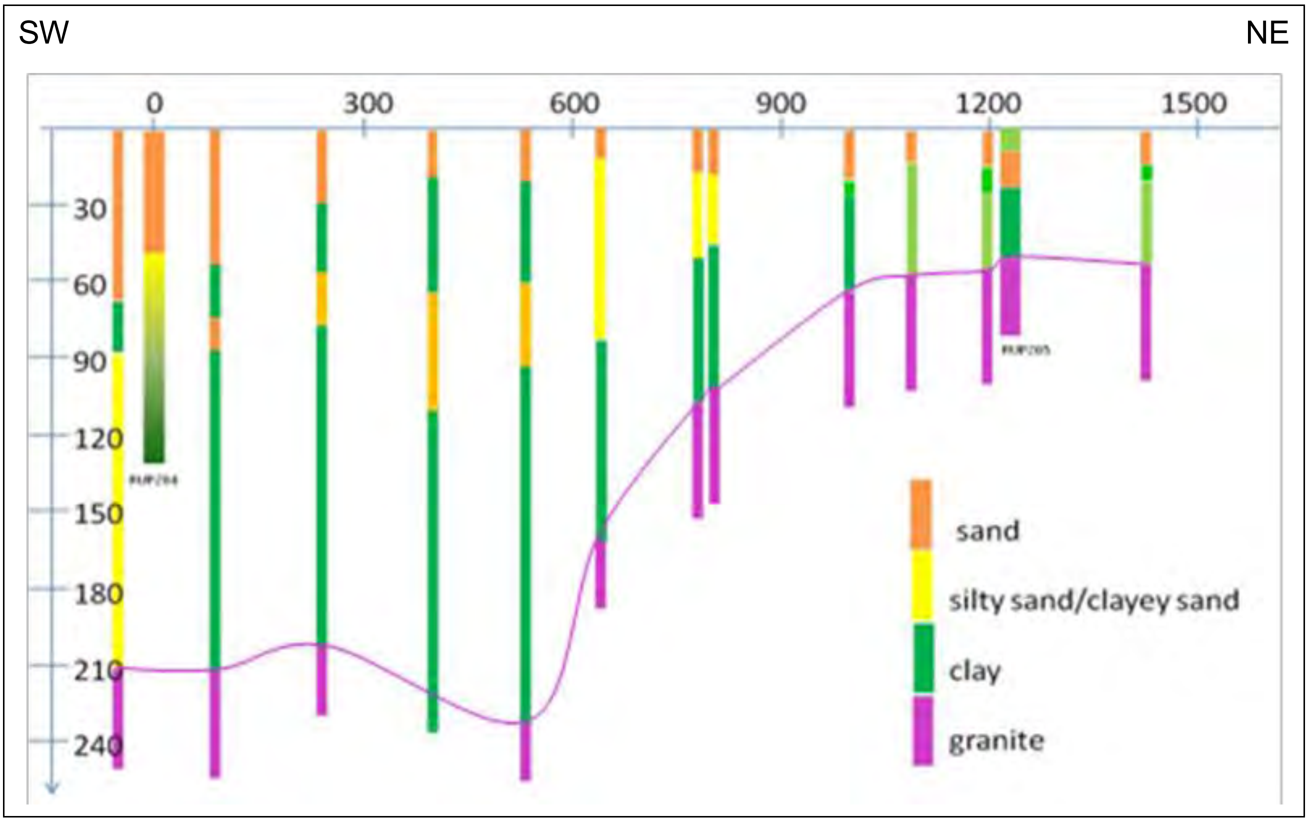

Figure 5.3: Interpretation of a TEM profile in Rumonge perpendicular to the shoreline of Lake Tanganyika. The diagram (modified after NOELL, U. 2014) reveals strong evidence for the developing rift structure. Vertical offset of the basement (granite) coincide with lineaments visible on satellite imagery (Fig. 5.4).

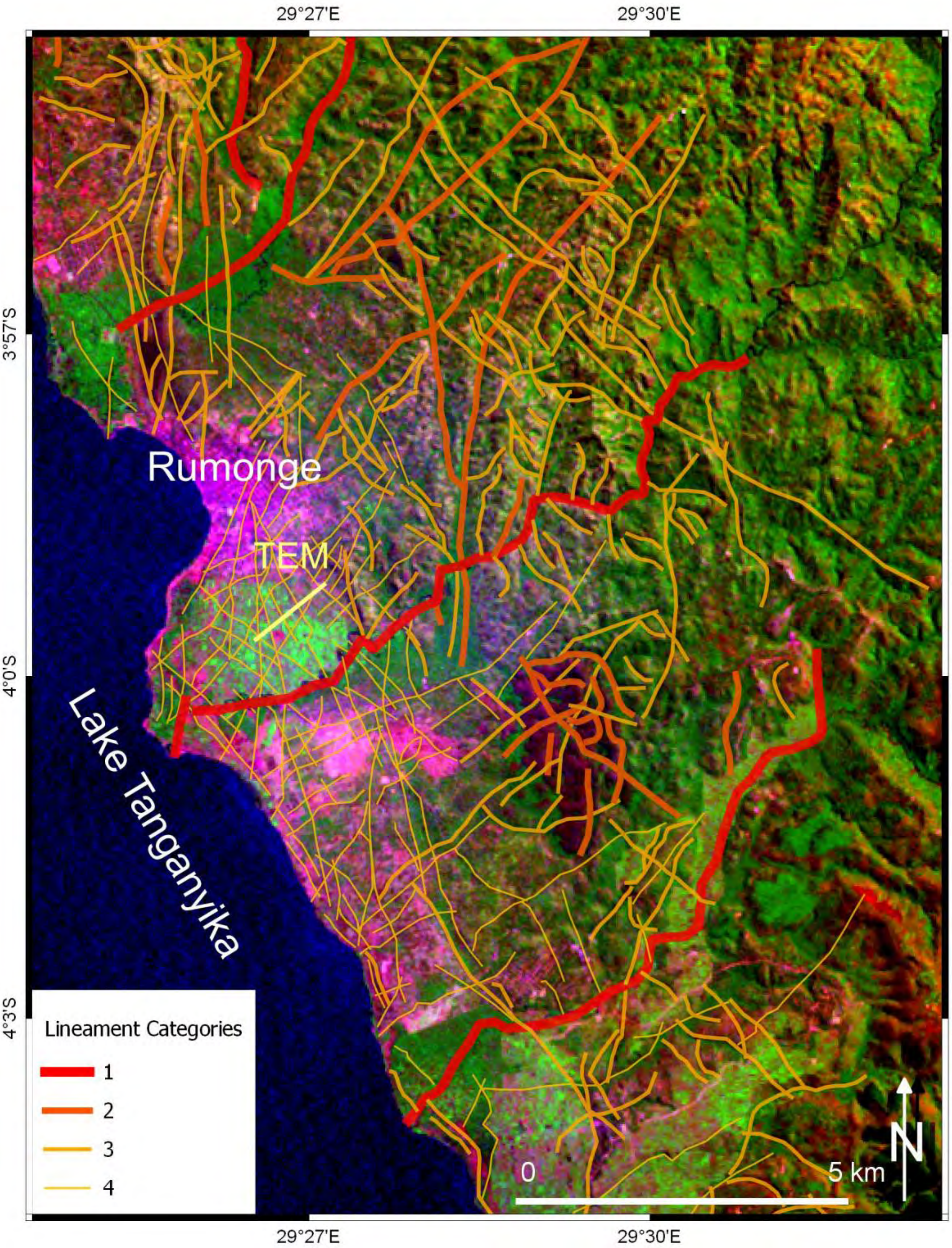

Figure 5.4: A TEM profile cuts several lineaments of Category 4 ("structures hardly or not visible on the ground but on remote sensing data") in Rumonge (Fig. 5.3). The vertical offset of the basement rocks up to approx. 70 metres is visible in the TEM profile. Cenozoic- and Quarternary sediments are also affected, which proves the existence of active faulting. Landsat TM bands 7,4,1 (RGB).

As faults of NE- and SE- strike directions seem to be still active with the ongoing rifting, it is very reasonable that they are open for groundwater migration.

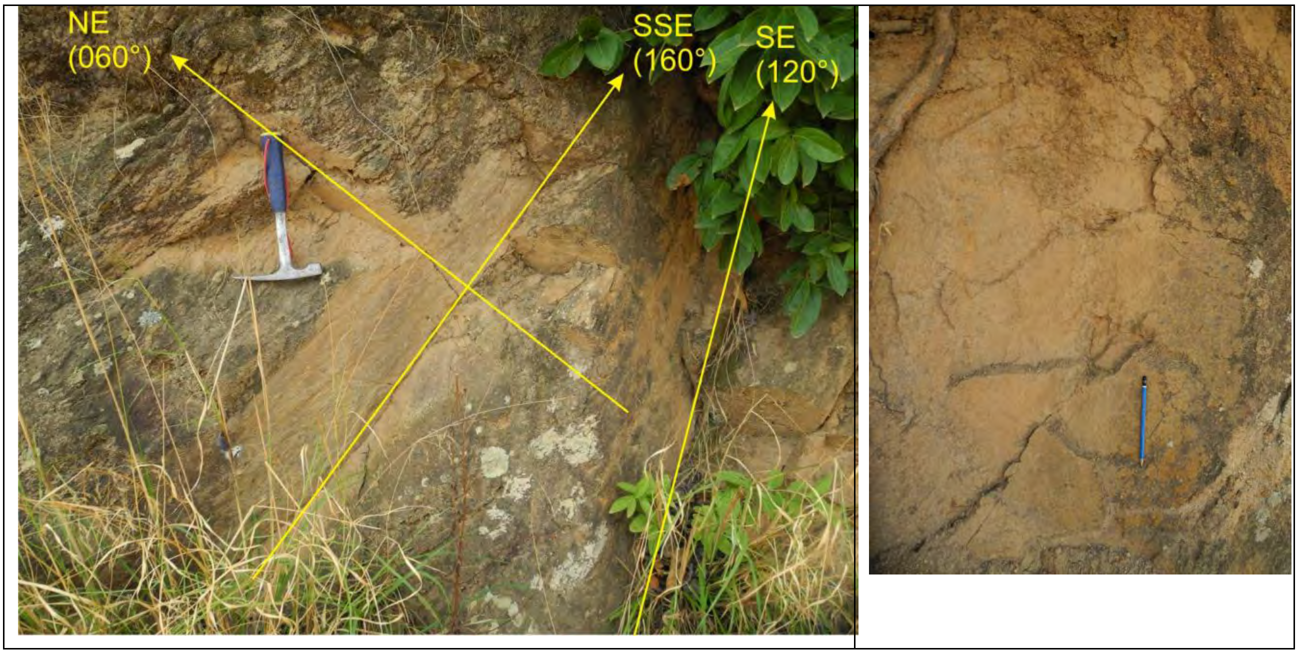

Figure 5.5: Left: (WP 85) Outcrop showing different joint planes with corresponding lineament directions at a small scale. Right: (WP 84) Tear-off edges show an upward-directed relative-movement of a former hanging wall.

Gitega:

In the area of Gitega (Fig. 2.3) the main structural trend is NW-SE. Lineaments are striking parallel to this trend (SE, app. 130°-170°) as well as in diagonal directions (NE 050°-060° and SE 110°-120°. Fig. 5.7).

These directions are generally the same as in Rumonge and can also be considered as reactivated in the Cenozoic and still active and thus open for groundwater migration. This assumption is strongly supported at a very productive well field south of Gitega which is situated in an area of intersecting lineaments (Fig. 5.6). These wells produce between 20 m^3/h and 70 m^3/h and in total more than 200 m^3/h (personal communication with Christian Tiberghien).

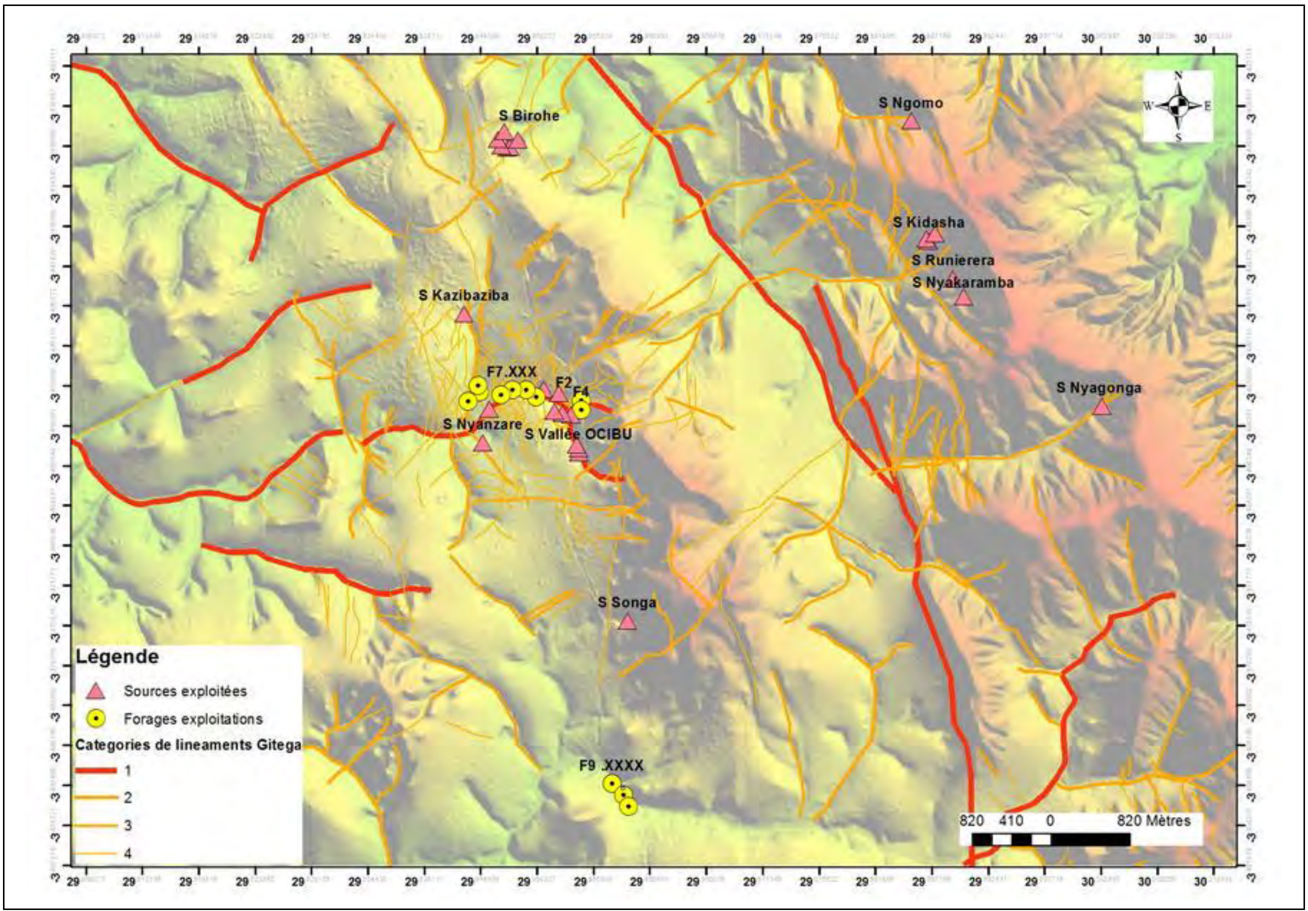

Figure 5.6: A very productive well field south of Gitega is situated in an area of intersecting lineaments. Lineaments can be considered as open for groundwater flow. Image: DEM from stereoscopic aerial photographs.

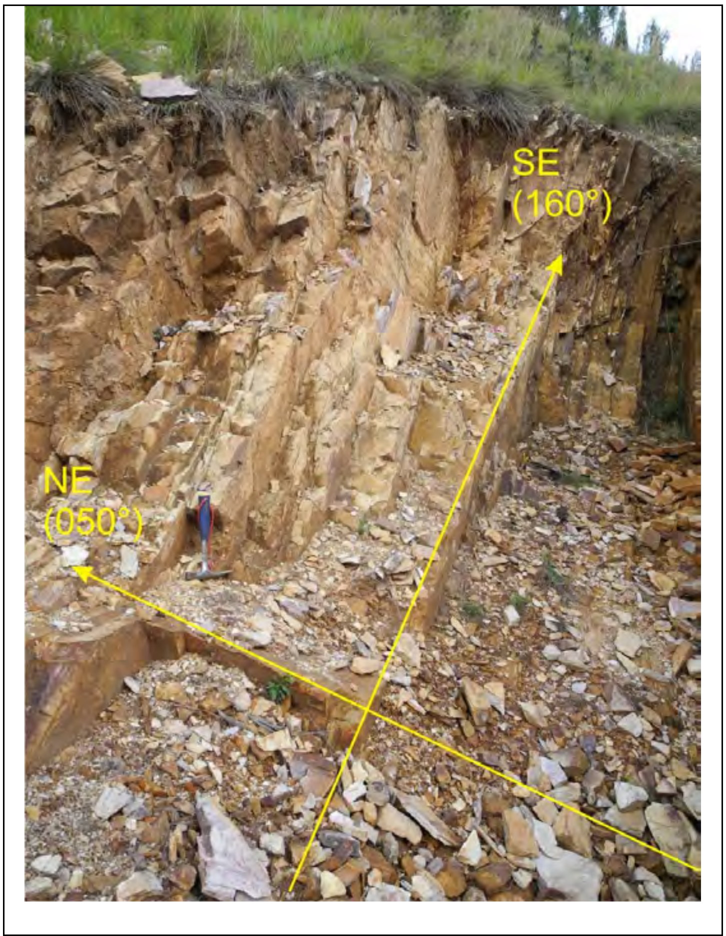

Figure 5.7: Steep dipping Precambrian quartzite (WP 53). Foliation and joints correspond to NE and SE striking lineaments.

Kirundo:

In the area of Kirundo (Figures 2.2 and 5.8) the main structural trend of the Kibaran Belt is NE-SW. Lineaments are striking parallel to this trend (NE 030°-050°) and in diagonal directions (SE 100°-160°).

The intrusive rocks (highly altered granite) and the surrounding metamorphites roughly show a circular structure (Fig. 5.8). Nevertheless, the lineaments of this unit follow the same directions as in the NE-SW-trending metamorphites (Fig. 5.8).

These directions strongly correspond to the Cenozoic conjugate faults described for Rumonge and Gitega before. It is thus reasonable, that these faults and joints are open for groundwater migration. This assumption is proven at many locations where operating wells are established.

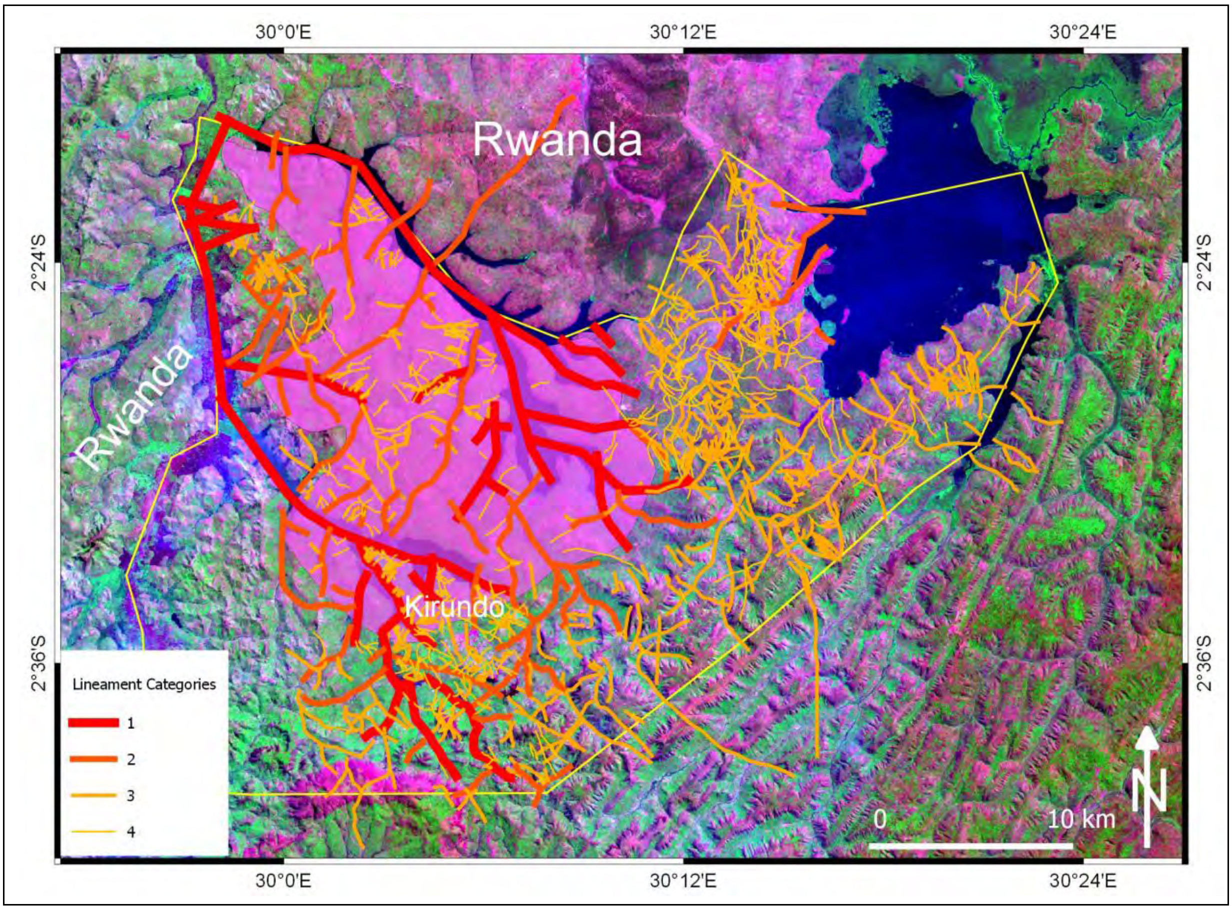

Figure 5.8: Kirundo area: different lithology does not affect the course of faults and joints significantly. Lineament strike directions are the same in folded metamorphites as well as in highly altered granite (pink polygon). Landsat TM bands 7,4,1 (RGB).

6 Lineaments

The mapped lineaments were additionally classified according to their surface expressions. These expressions were termed as categories 1 to 4, which range from huge to very small.

1. First order valleys,
2. Secondary order valleys,
3. Lineaments visible in satellite images by means of minor topographic features,
4. Lineaments visible in satellite images - invisible in the field.

The visibility of lineaments of category 4 is possible due to gentle differences in soil moisture, soil composition and distinctive features of vegetation tracing soil-burden lineaments.

The highest potential for groundwater can be expected at intersecting open joint and faults, visible on satellite images as lineaments.

This assumption was verified at many locations visited during field work.

6.1 Lineament Maps and examples from fieldwork

The following chapter outlines lineament maps based on satellite image interpretation with examples of different lineament categories from field work (Figures 6.1 to 6.18).

Rumonge

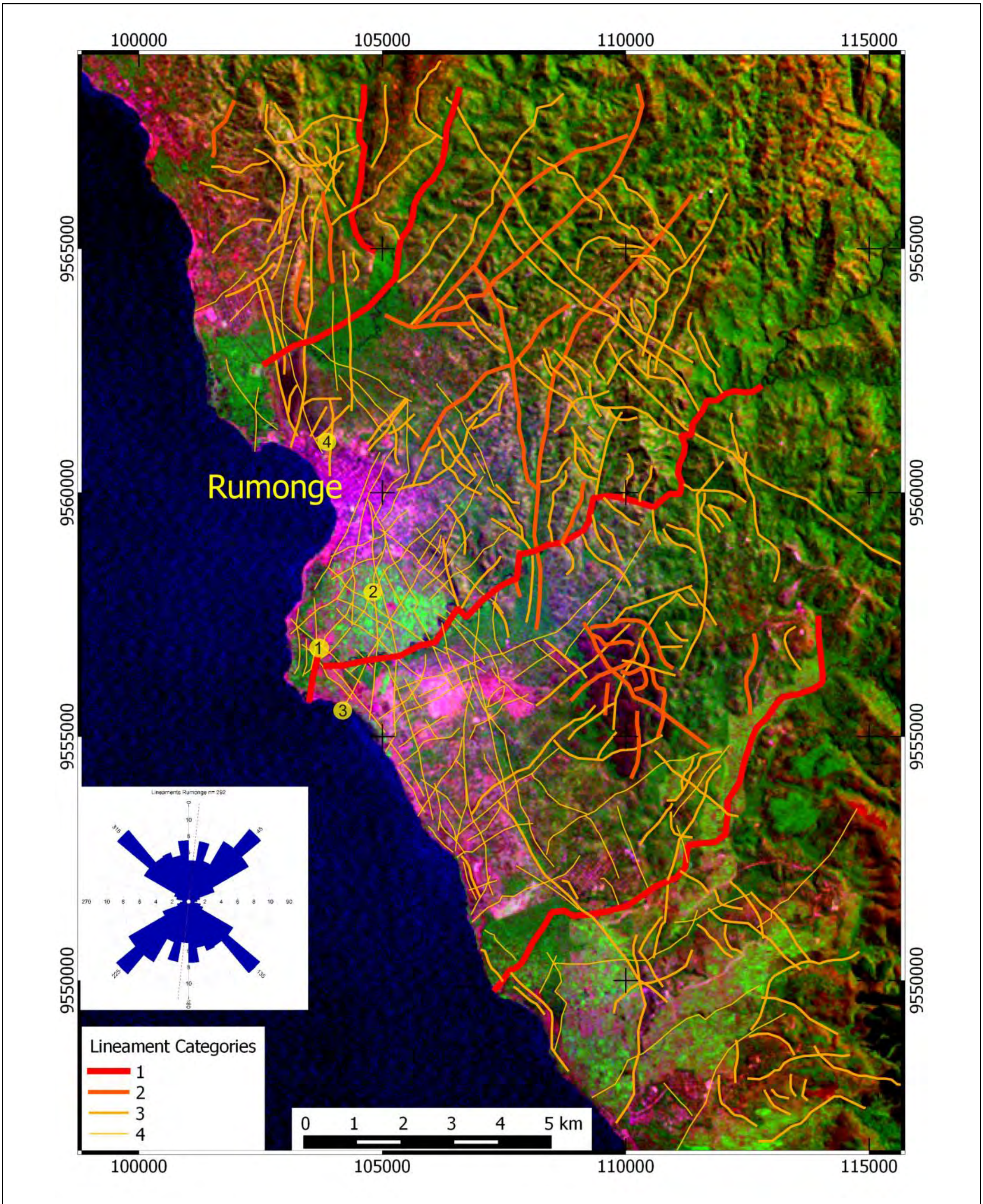

Figure 6.1: Lineament map of Rumonge area. Inset shows rose diagram with directions of mapped lineaments. Numbers 1 to 4 mark locations of field photos. Landsat TM bands 7,4,1 (RGB).

Figure 6.2: View from 180° to 320° (WP 80): The river bed corresponds to a lineament of Category 1. Other lineaments are not visible on the ground. The angular course of the river traces different lineament directions of the basement.

Figure 6.3: View from 170° to 090° (over South, WP 82): No lineaments of Category 4 are visible in this plantation.

Figure 6.4: View from 230° to 360° (WP 79): No shore-parallel lineaments of Category 4 are visible in this plantation.

Figure 6.5: View from 260° to 090° (over North, WP 83): Lineaments of Category 3 form clearly visible valleys which are here corresponding to faults.

Gitega

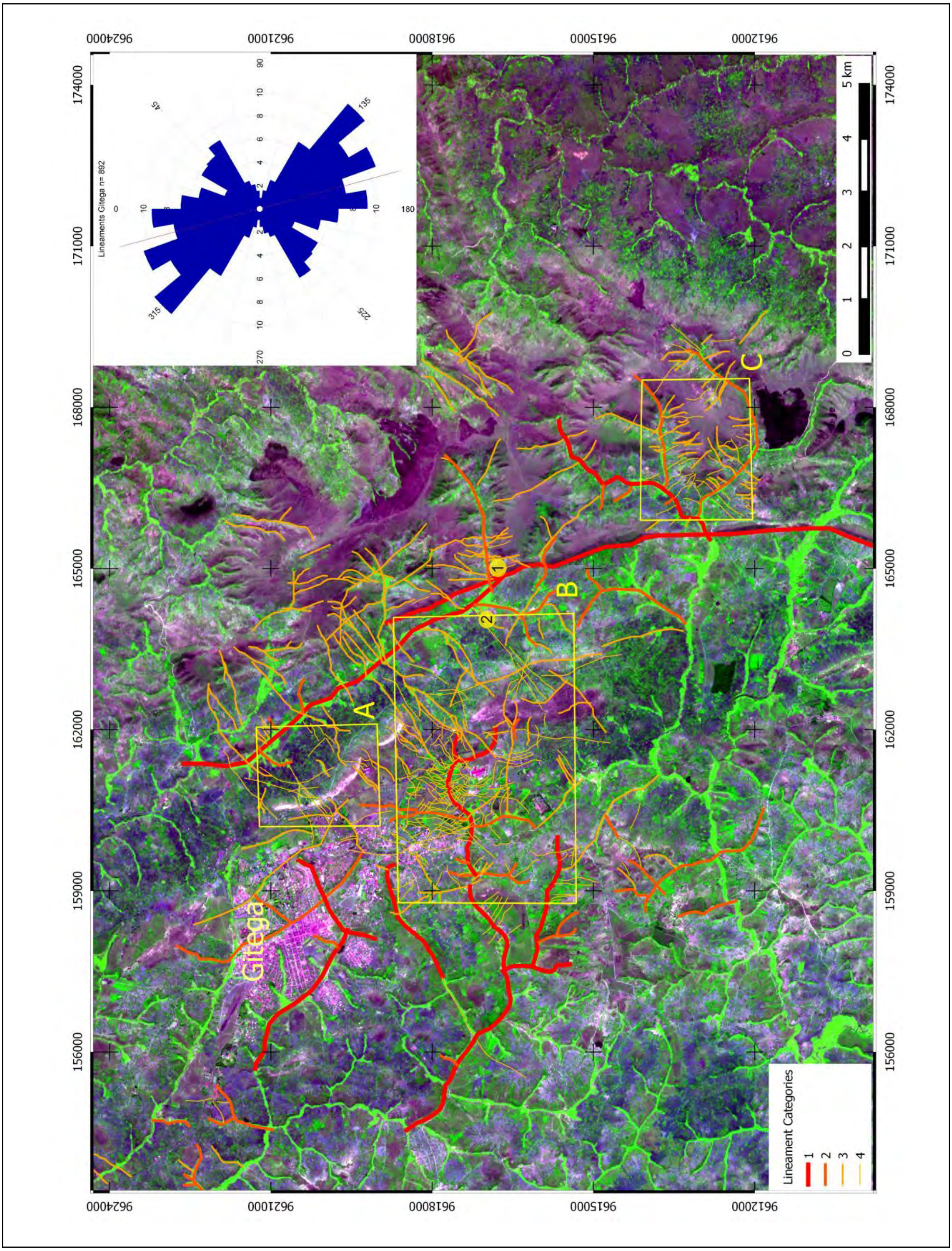

Figure 6.6: Overview of categorised lineaments around Gitega (selection) and locations of three areas of special interest (yellow rectangles, detailed mapping) A, B and C (Figures 6.9-6.11). The inset shows a rose diagram with directions of mapped lineaments. SPOT bands 2,3,1 (RGB).

Figure 6.7: View from 260° to 030° (WP 54): Lineaments of Category 2 (side valley in foreground) and Category 1 (main valley in background) are represented by major valleys.

Figure 6.8: Well on a lineament of Category 3. View to NE towards a main valley of Category 1 (WP 56).

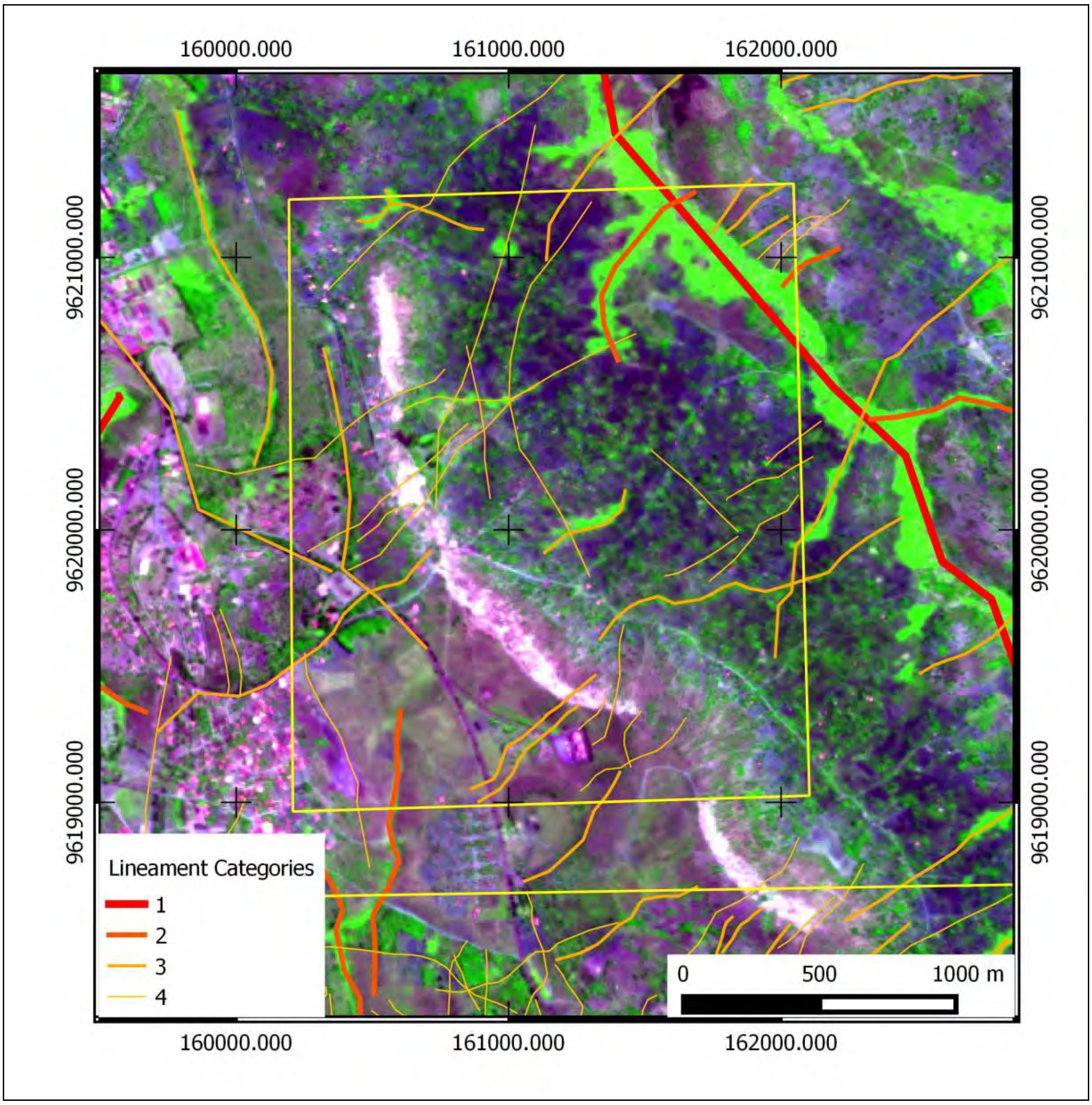

Figure 6.9: Lineaments of Gitega Area A. SPOT bands 2,3,1 (RGB).

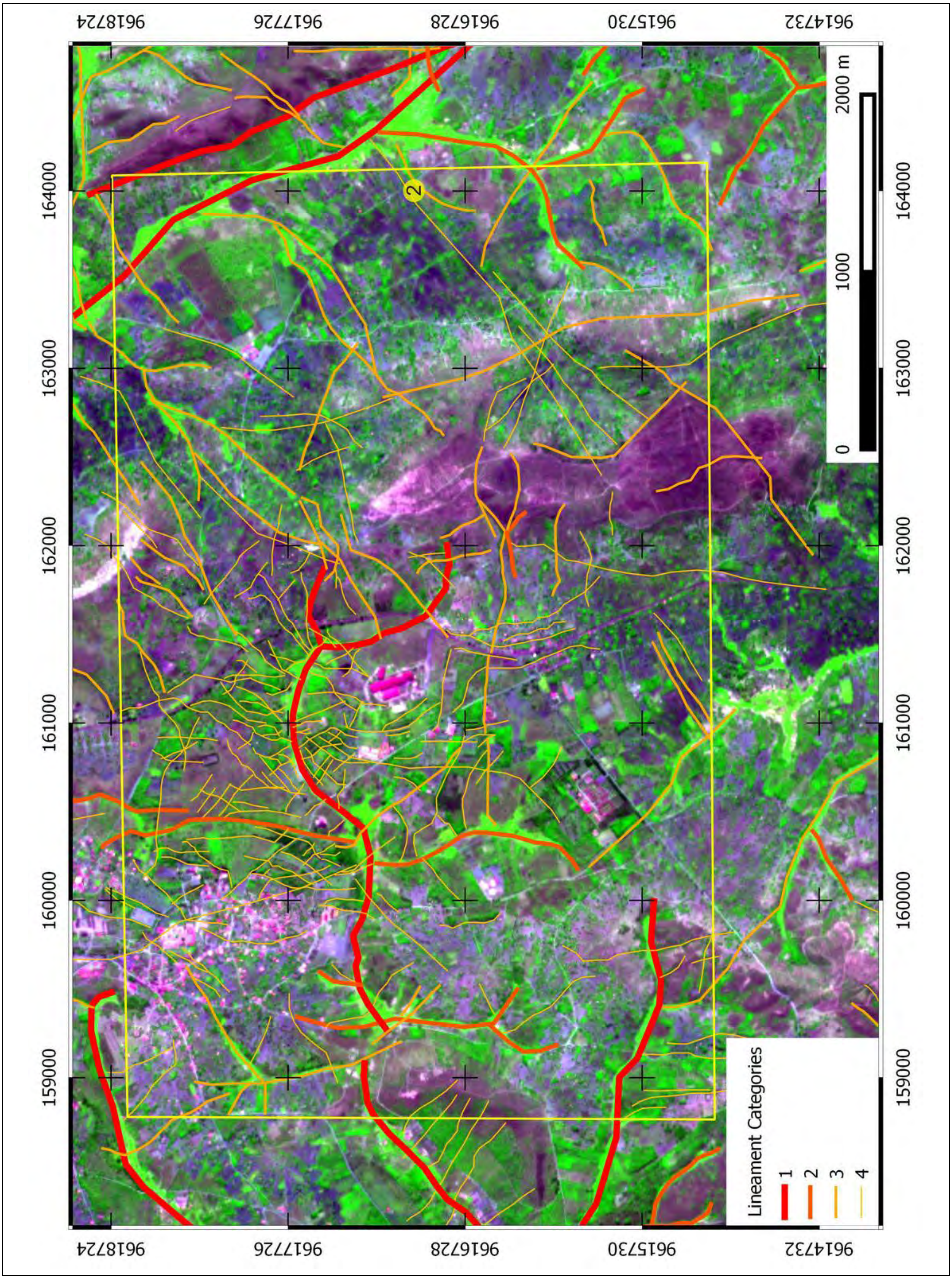

Figure 6.10: Lineaments of Gitega Area B. Number 2 marks the location of field photo. SPOT bands 2,3,1 (RGB).

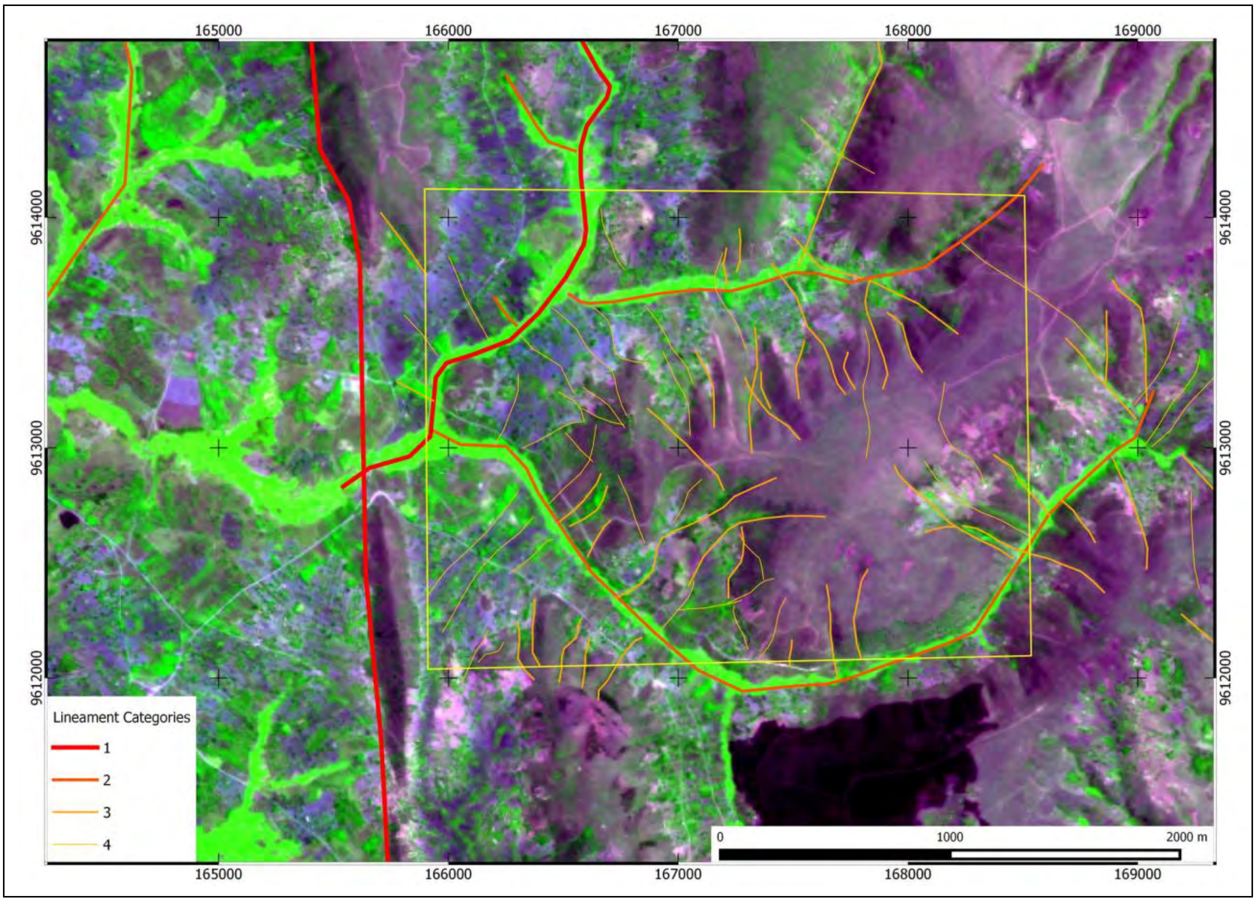

Figure 6.11: Lineaments of Gitega Area C. SPOT bands 2,3,1 (RGB).

Kirundo

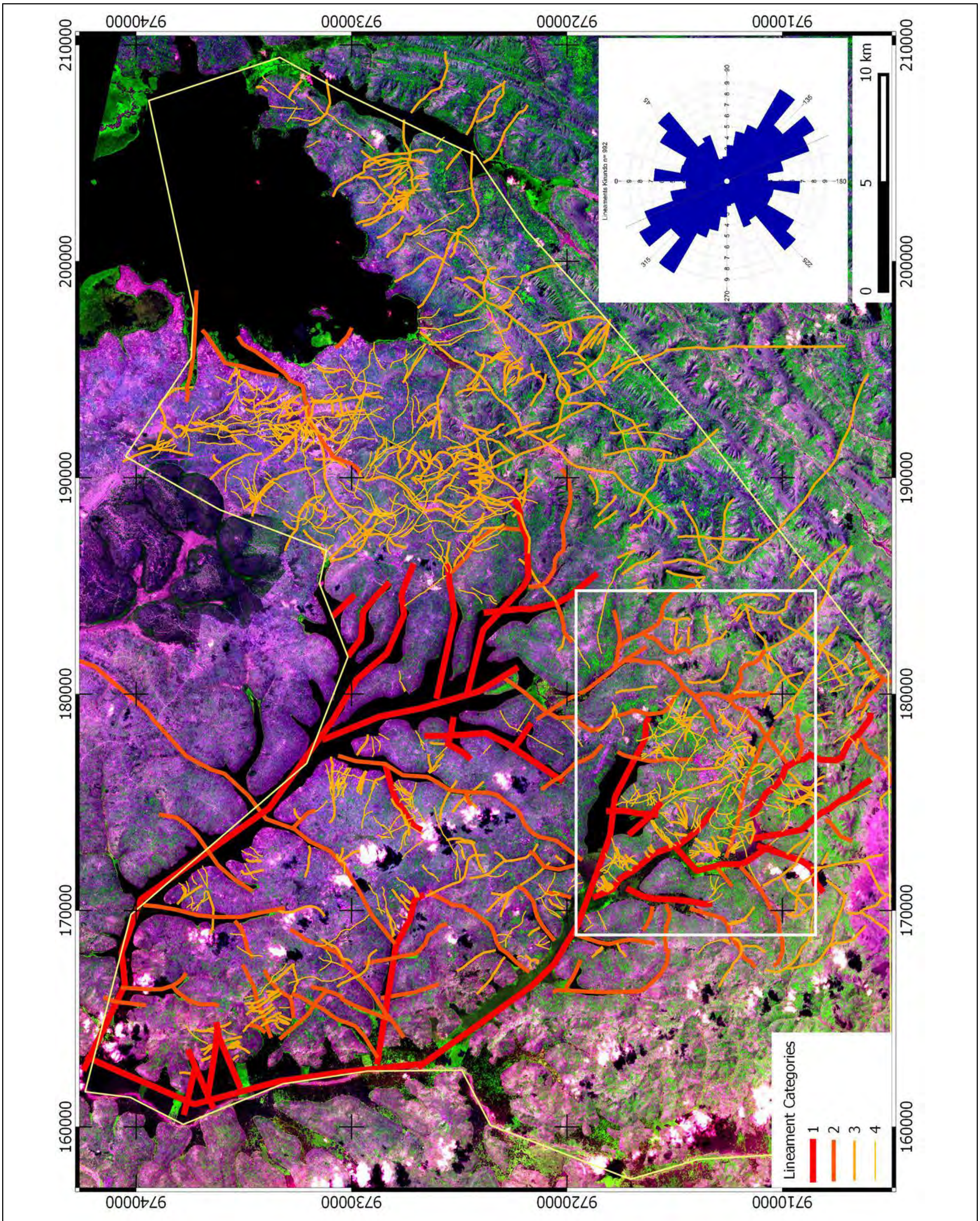

Figure 6.12: Lineament map of Kirundo area. The inset shows a rose diagram with directions of the mapped lineaments. The white rectangle outlines the area of figure 6.13. SPOT bands 2,3,1 (RGB)

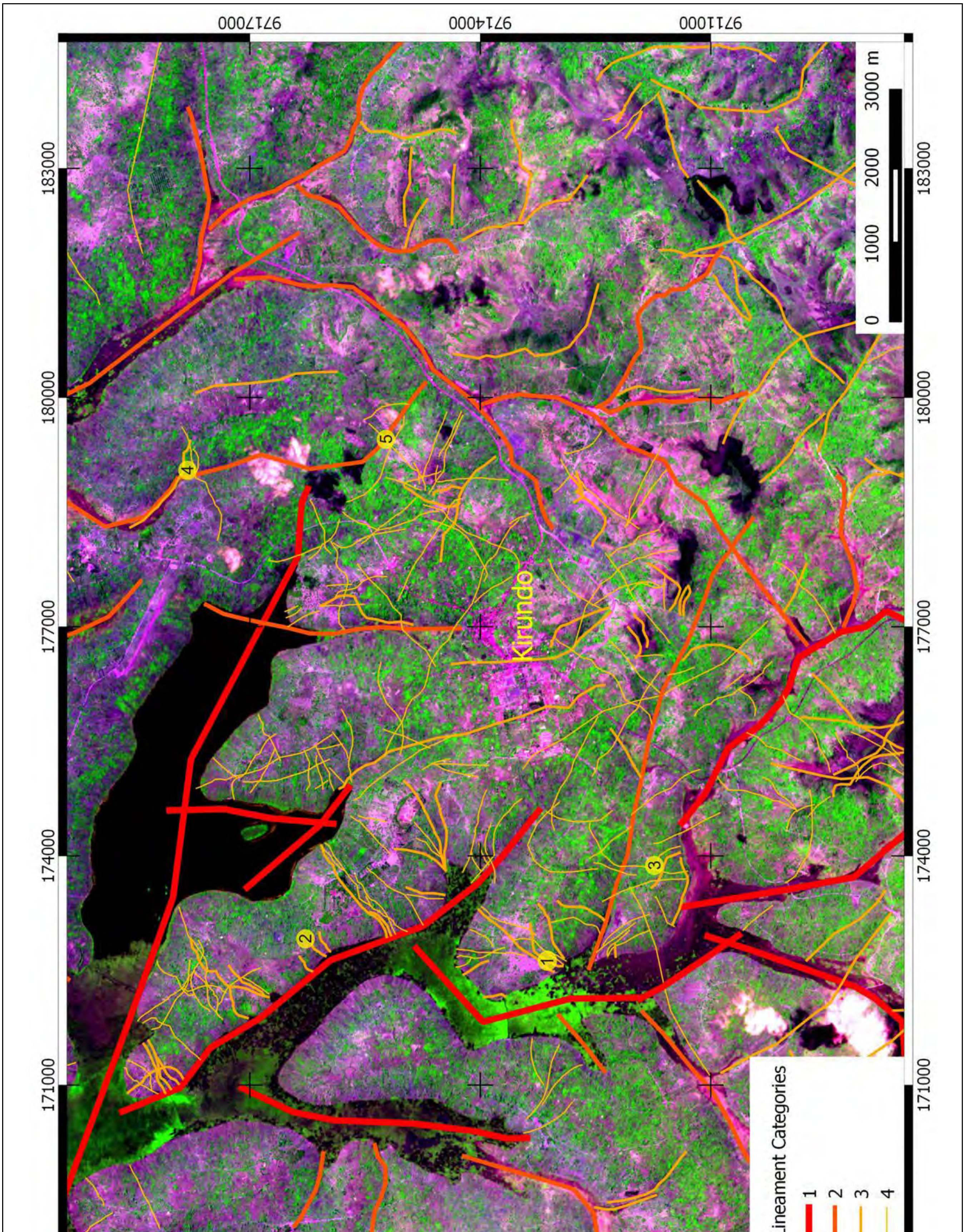

Figure 6.13: Subset of Kirundo lineament map (Fig. 6.12). Numbers 1 to 5 mark locations of field photos. SPOT bands 2,3,1 (RGB).

Figure 6.14: Above: View from 170° to 250° (WP 03): Valley bottoms follow lineaments of Category 1 and are filled with swamps. Lineaments of minor categories are not visible from this position. Below: Transportation between villages separated by swamps (WP 01).

Figure 6.15: View from 120° to 230° (WP 16): Valley bottoms represent lineaments of Category 1. Lineaments of Category 3 are visible as minor depressions running towards the main valley.

Figure 6.16: View from 050° to 170° (WP 09): Lineament of Category 4 is not visible in this plantation. Lineament of Category 3 is almost invisible and can be presaged by a minor depression in the background (right edge).

Figure 6.17: Wells at an intersection of minor lineaments (Category 3 and 4) prove that these lineaments are open for groundwater migration. WP 26, view to 060°.

Figure 6.18: View from 320° to 110° (WP 21). A lineament of Category 2 is divided by a ridge. Schist foliation is dipping steep (85°) to SE. A well in the NW supplies only little- while a well in the SE delivers plenty of water. The most probable reason is additional groundwater contribution by open foliation in this area.

Table 1: Numeric distribution of categorized lineaments within the study areas and their percentage. Lineaments of Category 4 represent the majority of all mapped and classified lineaments.

Category	Kirundo	Gitega	Rumonge	Total amount of categorized lineaments	% of total
1	29	11	5	45	2,55
2	56	39	21	116	6,56
3	417	174	161	752	**42,56**
4	493	256	105	854	**48,33**
Σ	995	480	292	**1767**	100

7 Contamination

Many of the detected lineaments can be considered as open pathways for groundwater migration. For this reason contamination can take place along these vectors. In the study areas pit latrines appear to be the most common source of contamination (Figures 7.4 to 7.7) resulting in high bacteria content of wells. Besides that, mining activities and petrol storage can also be a risk for water pollution at some places (Figures 7.1 to 7.3).

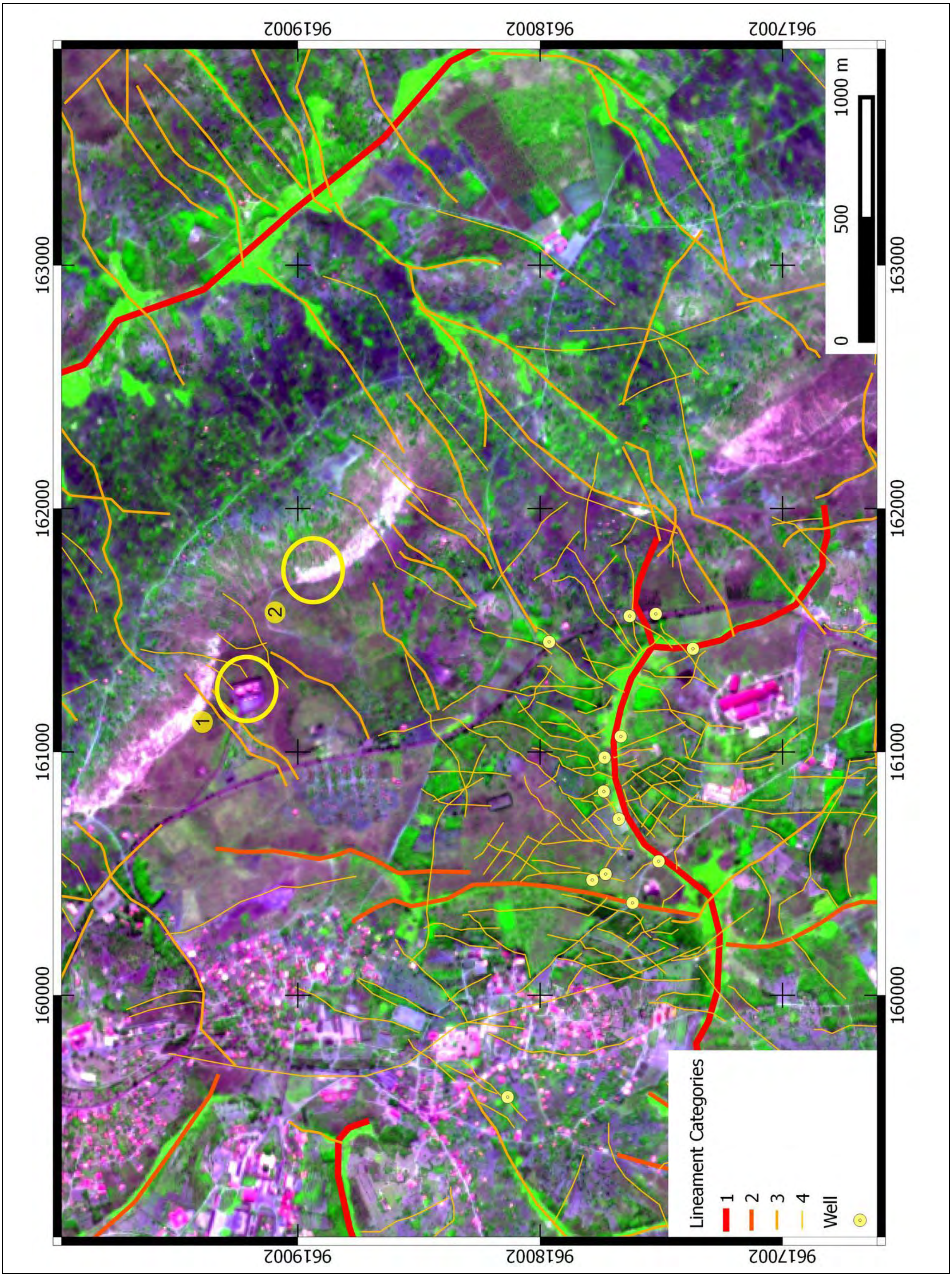

Figure 7.1: Sites of possible contamination at Gitega. Numbers 1 and 2 and yellow circles mark the locations of field photos. SPOT bands 2,3, (RGB).

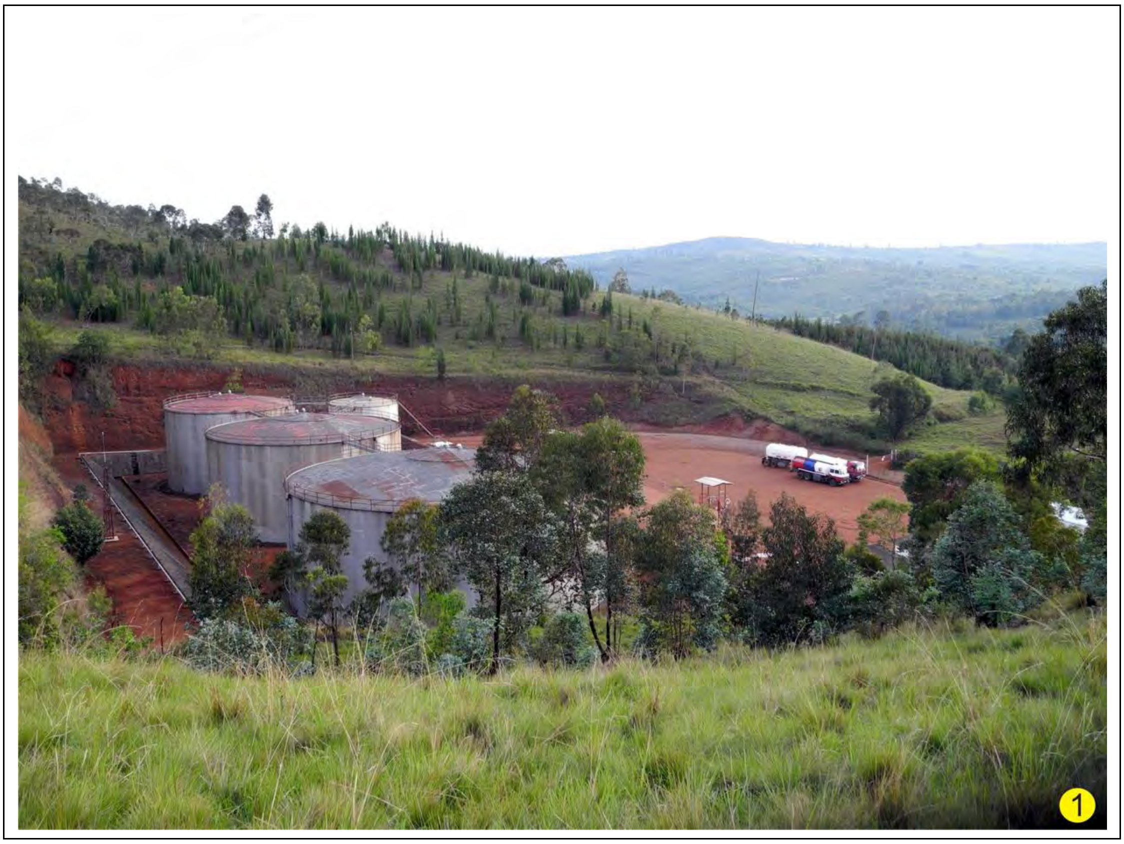

Figure 7.2: View to SE onto a petrol storage. Leakage could possibly cause contamination through open faults at wells downstream.

Figure 7.3: View to the east. Artisanal mining activities along the slopes are visible on satellite images as whitish areas. Sludge from the mines has the potential for water contamination of wells situated downhill.

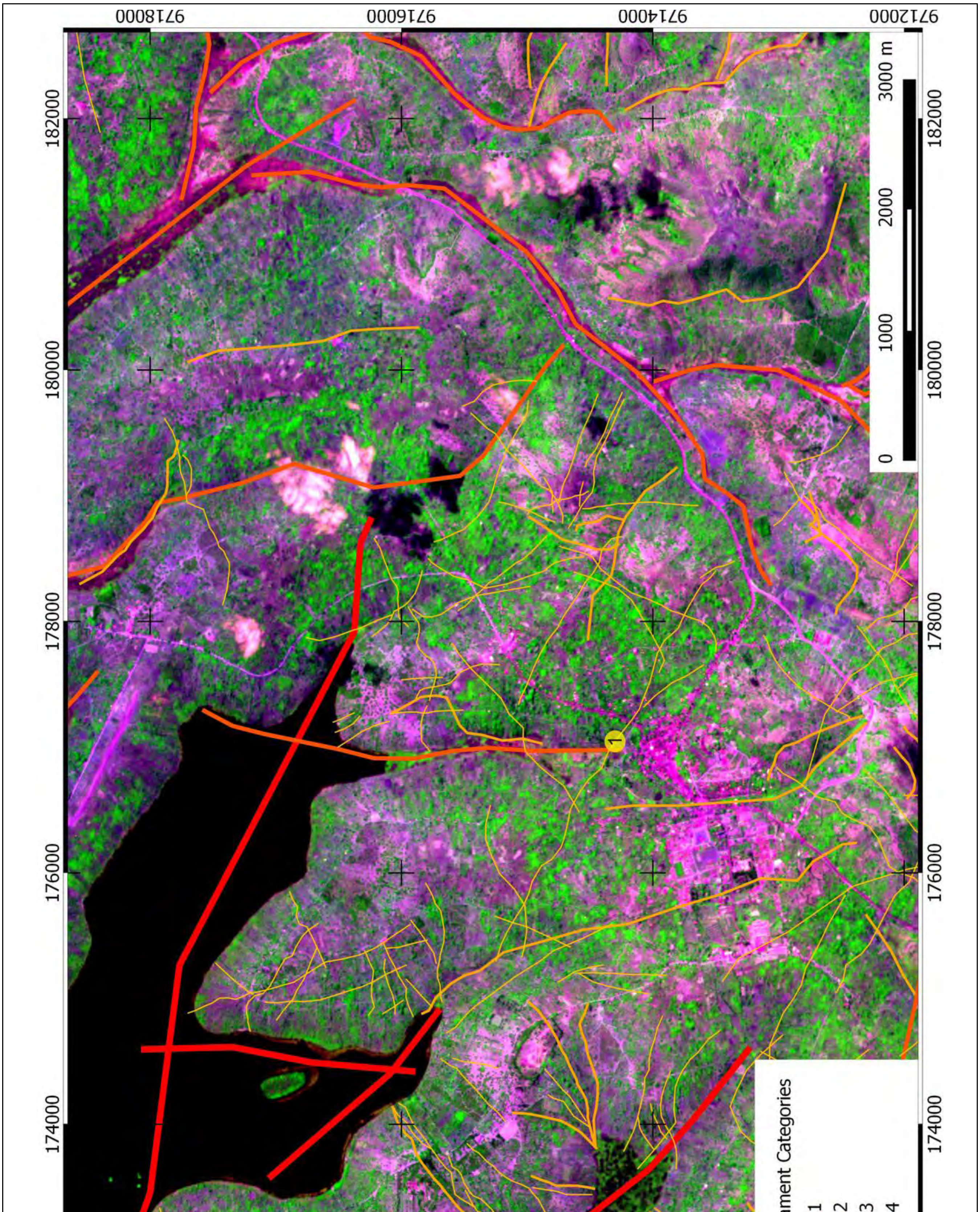

Figure 7.4: Possible water contamination site at Kirundo. Number 1 marks the location of field photo. SPOT bands 2,3,1 (RGB).

Figure 7.5: View to the south (WP 11). High bacteria content of these wells at this pump station may be caused by pit latrines directly uphill. The pond directly to the right functions also as a car wash. A small slaughterhouse nearby may cause further contamination.

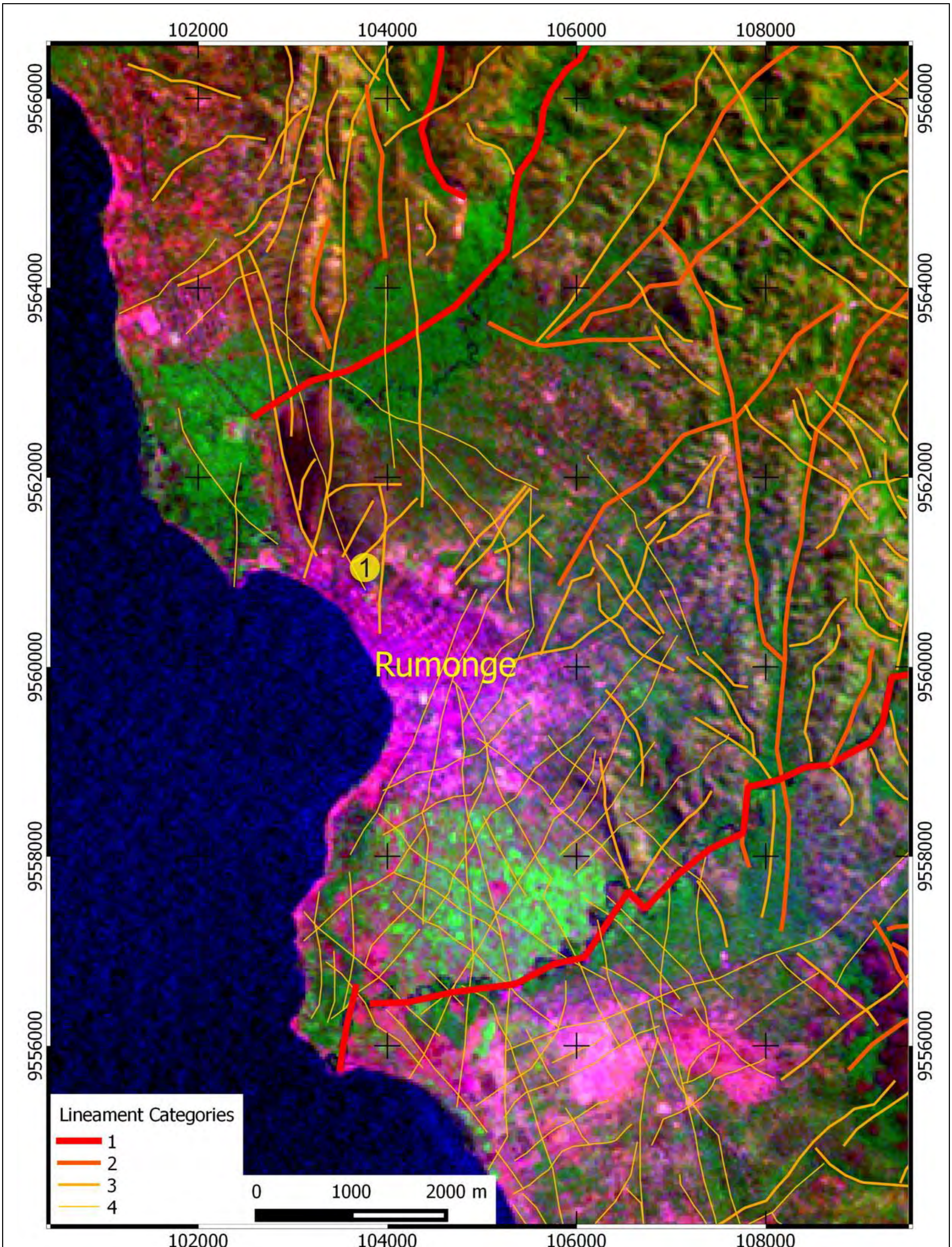

Figure 7.6: Site of possible water contamination at Rumonge. Number 1 marks the location of field photo. Landsat TM bands 7,4,1 (RGB).

Figure 7.7: View to NE (WP 83). Pit latrines in this fault may cause water contamination. Right: sealed toilets nearby are a good step towards a better solution.

8 Conclusions

The results of the lineament mapping and conducted field work can be characterized by the following points:

- The majority of categorized lineaments is only visible in enhanced multispectral satellite images (“Category 4”; 48,33 %, tab. 1) and not on the ground. This shows that remote sensing techniques are an important tool.
- Compared to existing lineament maps, the new maps could be improved significantly by using high and medium resolution multispectral satellite images.
- Vast parts of the study areas are covered by thick soil, which makes direct detection of small tectonic features on the ground impossible. Most “Category 4” structures become detectable in satellite images by tiny differences in soil moisture and vegetation.
- Most of the mapped lineaments appear to be in the Cenozoic (re-) activated structures and appear to be open for groundwater migration at many locations.
- The highest groundwater potential is at lineament intersections. This is proven by already existing- and new drilled wells at those locations.
- Pit latrines seem to be the major factor for groundwater contamination, which can easily take place along the open pathways supplied by tectonic structures.

9 References

BARRAT, JM., MARDHEL, V., GUTIERREZ, A., PINSON, S. (2011): Cartes des Potentialités en eaux souterraines du Burundi. Avec la collaboration de E. Buscarlet et S. Lallier. BRGM/RC- 59751-FR.

CHOROWICZ, J. ET AL. (1990): The evaluation of satellite imagery and field spectro-radiometer data for the study of the lithology and the ancient and reactivation tectonics in the vicinity of the East African Rift. ISPRS Journal of Photogrammetry and Remote Sensing, 45, 355-381, Elsevier, Amsterdam.

CLAESSENS, W. ET KARAYENGA, D. (1986): Carte géologique du Burundi au 1/100.000. Feuille Muyinga S3/30 SW. Ministère des Travaux Publics, de l´Energie et des Mines, Bujumbura, Burundi.

CLAESSENS, W. ET THEUNISSEN, K. (1988): Carte géologique du Burundi au 1/100.000. Feuille Gitega S4/29 NE. Ministère des Travaux Publics, de l´Energie et des Mines, Bujumbura, Burundi.

KARAYENGA, D. (1989): Carte géologique du Burundi au 1/100.000. Feuille Busoni S3/29 NE, S3/30 NW et S3/30 NE. Ministère des Travaux Publics, de l´Energie et des Mines, Bujumbura, Burundi.

NOELL, U. (2014): Report on the Geophysical measurements to support the Technical Cooperation Project in Burundi: Management and Protection of Groundwater Resources as part of the Programme Sectoriel Eau (ProSecEau); BGR, Hannover, Germany.

RUMVEGERI, B. T. (1991): Tectonic significance of Kibaran structures in Central and Eastern Africa. Journal of African Earth Sciences, 13, No. 2, 267-276, Pergamon Press.

TACK, L., WINGATE, M.T.D., DE WAELE, B., MEERT, J., BELOUSOVA, E., GRIFFIN, B., TAHON, A., FERNANDEZ-ALONSO, M. (2010): The 1375 Ma „Kibaran event“ in Central Africa: Prominent emplacement of bimodal magmatism, under extensional regime. Precambrian Research, 180, 63-84.

THEUNISSEN, K. (1986): Carte géologique du Burundi au 1/100.000. Feuille Rumonge S4/29 SW. Ministère des Travaux Publics, de l´Energie et des Mines, Bujumbura, Burundi.

VAN DEN HAUTE, P. (1984): Fission-track ages of apatites from the Precambrian of Rwanda and Burundi: relationship to East African rift tectonics. Earth and Planetary Science Letters, 71, 129-140, Elsevier, Amsterdam.

Appendix

Waypoints of measurements and field photos as mentioned in figures. The datum of coordinates (UTM zone 36 S) is WGS84.

WP No	UTM X	UTM Y	Height [m] asl	Date
1	172199.06	9713713.09	1378.4	09.10.2012 10:04
2	172521.82	9713326.08	1405.3	09.10.2012 10:27
3	172608.26	9713163.36	1410.1	09.10.2012 10:53
4	173184.54	9712577.99	1410.1	09.10.2012 11:18
5	173396.61	9712324.80	1388.5	09.10.2012 11:47
6	173223.71	9712291.34	1372.9	09.10.2012 11:59
7	173414.94	9711854.82	1428.9	09.10.2012 12:21
8	173447.60	9711743.19	1426.2	09.10.2012 12:42
9	173865.84	9711701.05	1427.9	09.10.2012 13:07
10	177030.60	9714183.35	1390.9	09.10.2012 15:59
11	176960.46	9714223.99	1377.9	09.10.2012 16:13
12	177148.54	9715014.32	1383.9	09.10.2012 16:43
13	177368.20	9714860.80	1417.1	09.10.2012 16:59
14	172099.95	9717935.91	1409.9	10.10.2012 09:28
15	172452.04	9717152.17	1459.4	10.10.2012 09:40
16	172832.20	9716260.86	1416.6	10.10.2012 09:56
17	174347.58	9715254.73	1429.8	10.10.2012 10:19
18	175707.87	9715220.78	1445.9	10.10.2012 11:13
19	175007.59	9716800.35	1408.7	10.10.2012 11:46
20	178225.68	9715936.40	1399.1	10.10.2012 14:59
21	179439.44	9715108.71	1474.3	10.10.2012 15:25
22	179149.46	9717909.61	1409.9	11.10.2012 08:39
23	179154.39	9717811.35	1402.9	11.10.2012 08:47
24	179134.99	9717791.05	1395.5	11.10.2012 09:00
25	179074.99	9717780.42	1375.3	11.10.2012 09:11
26	179067.72	9717773.82	1374.6	11.10.2012 09:14
27	171309.04	9724987.88	1388.7	11.10.2012 10:35
28	171537.64	9724760.95	1394.3	11.10.2012 10:50
29	171477.70	9724233.03	1461.1	11.10.2012 11:19
30	171520.82	9724150.17	1467.6	11.10.2012 11:23
31	173770.95	9727449.81	1412.5	11.10.2012 12:30
32	174018.11	9727283.43	1375.0	11.10.2012 12:37
33	174046.37	9727281.99	1373.6	11.10.2012 12:40
34	173368.06	9726069.09	1388.5	11.10.2012 13:05
35	175557.21	9731165.72	1446.7	11.10.2012 13:44
36	176540.36	9730900.62	1405.6	11.10.2012 14:07
37	177079.90	9730972.84	1358.9	11.10.2012 14:27
38	177056.63	9730927.86	1358.7	11.10.2012 14:35
39	177074.70	9730830.65	1359.4	11.10.2012 14:41

WP No	UTM X	UTM Y	Height [m] asl	Date
40	177012.91	9730795.83	1360.6	11.10.2012 14:58
41	172623.67	9730101.87	1376.5	11.10.2012 15:57
42	172268.46	9730500.75	1356.3	11.10.2012 16:24
43	172305.66	9730552.12	1352.7	11.10.2012 16:33
44	191190.68	9737647.03	1427.4	12.10.2012 10:06
45	192254.09	9738657.46	1386.3	12.10.2012 10:47
46	191780.39	9738813.89	1492.1	12.10.2012 11:41
47	191509.67	9739033.81	1516.8	12.10.2012 12:00
48	191487.11	9739026.10	1516.8	12.10.2012 12:14
49	191793.79	9738160.23	1413.7	12.10.2012 12:48
50	192844.94	9732168.28	1342.6	12.10.2012 13:23
51	188986.21	9734532.57	1389.9	12.10.2012 14:28
52	189433.46	9734510.69	1428.4	12.10.2012 14:41
53	164826.20	9616926.53	1708.1	15.10.2012 16:10
54	164851.35	9616927.49	1718.0	15.10.2012 16:27
55	164265.63	9616651.34	1691.6	15.10.2012 16:42
56	164073.46	9616978.74	1699.7	15.10.2012 16:44
57	163032.32	9617913.78	1724.0	15.10.2012 16:55
58	163189.36	9618821.30	1656.9	15.10.2012 17:00
59	161730.64	9619546.75	1702.1	15.10.2012 17:16
60	163753.02	9619411.86	1691.3	16.10.2012 13:39
61	163655.43	9619644.06	1722.3	16.10.2012 13:53
62	162788.82	9617345.48	1795.6	16.10.2012 14:37
63	162004.37	9618225.62	1752.1	16.10.2012 14:58
64	159927.09	9619415.41	1724.2	16.10.2012 15:09
65	157101.74	9618829.34	1684.6	16.10.2012 15:26
66	156982.60	9618828.50	1684.3	16.10.2012 15:28
67	155760.74	9618747.80	1659.3	16.10.2012 15:34
68	156253.92	9619707.06	1667.0	16.10.2012 15:47
69	156222.52	9619741.01	1667.8	16.10.2012 15:49
70	156205.68	9619780.71	1669.4	16.10.2012 15:50
71	156135.48	9619949.94	1663.9	16.10.2012 15:52
72	156157.36	9620058.51	1665.4	16.10.2012 15:53
73	156196.85	9620128.00	1667.3	16.10.2012 15:55
74	156284.92	9620150.96	1662.0	16.10.2012 15:56
75	155735.50	9620799.78	1662.7	16.10.2012 16:06
76	156735.17	9624356.02	1621.9	16.10.2012 16:47
77	105225.34	9556113.64	787.7	18.10.2012 12:51
78	104894.83	9555680.06	781.2	18.10.2012 13:05
79	104263.70	9555734.62	779.3	18.10.2012 13:22
80	103667.72	9556567.00	780.5	18.10.2012 16:29
81	104906.48	9556985.92	781.9	18.10.2012 16:55
82	104790.00	9557756.94	780.5	18.10.2012 17:03
83	103728.11	9561095.35	832.6	19.10.2012 08:49

WP No	UTM X	UTM Y	Height [m] asl	Date
84	108087.82	9562642.43	976.8	19.10.2012 09:47
85	108114.25	9562660.78	985.0	19.10.2012 10:04
Bore	103780.16	9558674.90	1729.3	18.10.2012 09:22
Bore1	103861.01	9558756.09	1722.6	18.10.2012 09:25
Borehole	103776.74	9558663.44	776.6	19.10.2012 08:19
Kongo-Nil Dev	116227.20	9635252.72	2163.6	04.10.2012 11:11

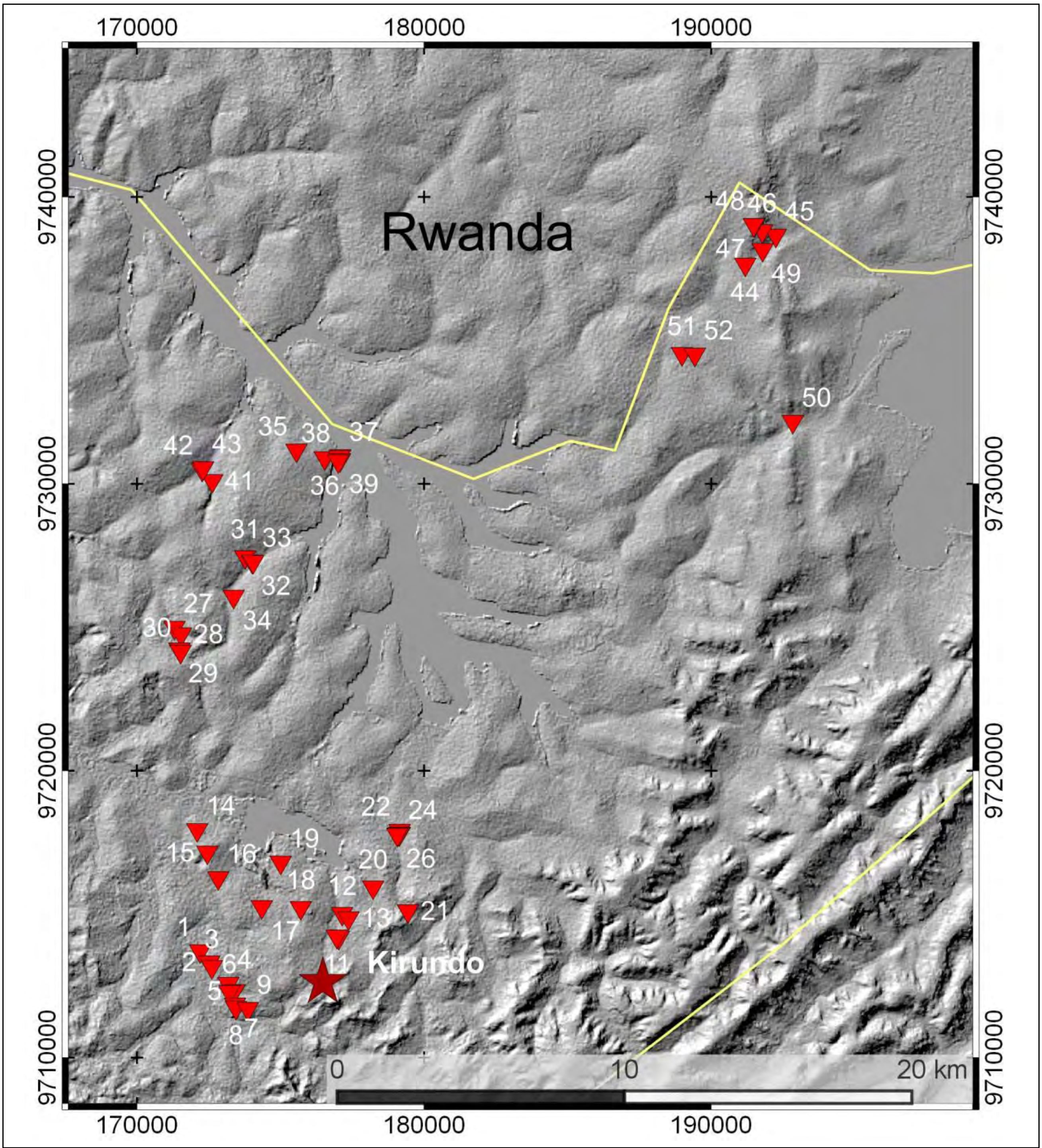

Waypoints of the working area 1 projected onto ASTER GDEM elevation model.

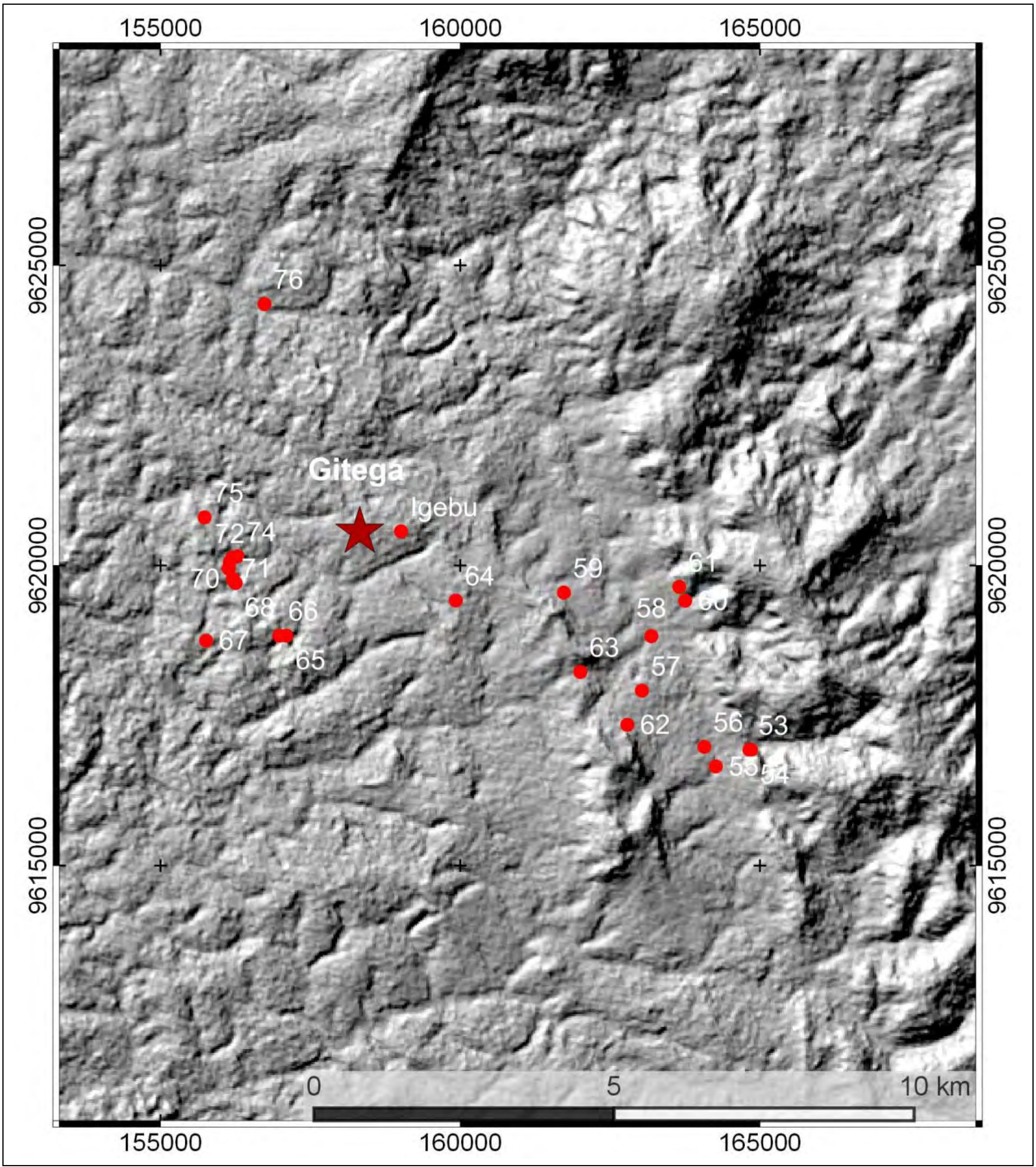

Waypoints of the working area 2 projected onto ASTER GDEM elevation model.

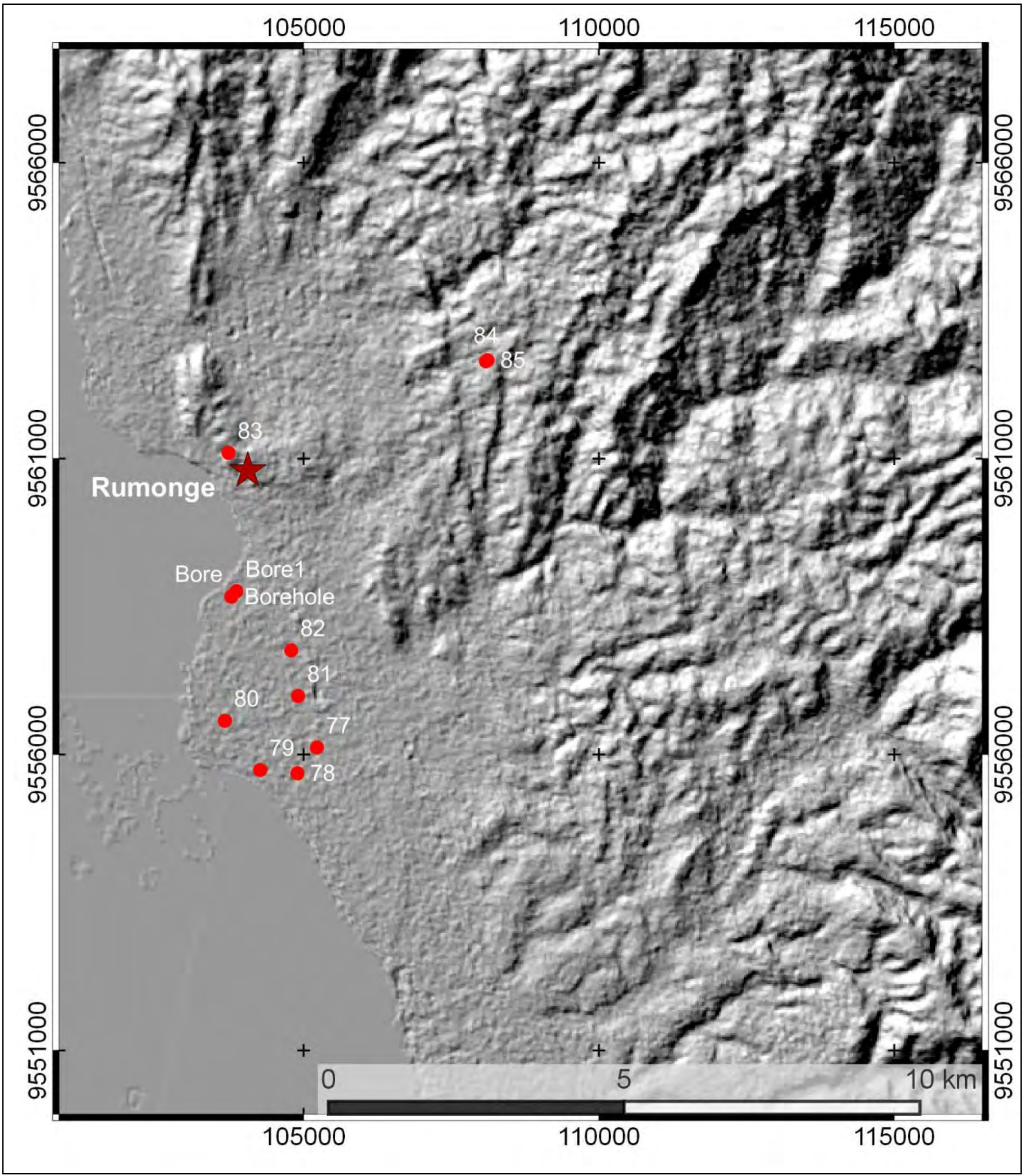

Waypoints of the working area 3 projected onto ASTER GDEM elevation model.